THE RELATION OF THE KINETICS OF CRYSTALLIZATION TO THE MECHANICAL PROPERTIES OF Li_2O-SiO_2 GLASS-CERAMICS

By

STEPHEN W. FREIMAN

A DISSERTATION PRESENTED TO THE GRADUATE COUNCIL OF
THE UNIVERSITY OF FLORIDA
IN PARTIAL FULFILLMENT OF THE REQUIREMENTS FOR THE
DEGREE OF DOCTOR OF PHILOSOPHY

UNIVERSITY OF FLORIDA
1968

Dedicated to my parents,

Dr. and Mrs. M. S. Freiman

ACKNOWLEDGEMENTS

The author would like to acknowledge the assistance of the many persons who contributed their time and effort toward a successful conclusion of this work.

The author would especially like to thank Dr. L. L. Hench (committee chairman), who through his help and guidance both during the experimental research and the preparation of this manuscript made this work possible. The author would also like to thank Dr. J. J. Hren for his many helpful suggestions and the other committee members, Dr. F. N. Rhines, Dr. R. G. Blake, and Dr. J. B. Conklin for their assistance.

The helpful advice provided by Dr. R. T. DeHoff and Dr. R. W. Gould concerning parts of this work is also greatly appreciated.

The author would also like to thank Mr. E. J. Jenkins for his help in obtaining many of the micrographs presented herein.

The support of the Graduate School of the University of Florida and the National Science Foundation during the course of this work is also acknowledged.

TABLE OF CONTENTS

LIST OF TABLES

LIST OF FIGURES

Abstract of Dissertation Presented to the Graduate Council
in Partial Fulfillment of the Requirements for the
Degree of Doctor of Philosophy

THE RELATION OF THE KINETICS OF CRYSTALLIZATION TO THE
MECHANICAL PROPERTIES OF Li_2O-SiO_2 GLASS-CERAMICS

By

Stephen W. Freiman

December, 1968

Chairman: L. L. Hench
Major Department: Metallurgy and Materials Engineering

Glass-ceramics are materials which are formed in the glassy state and subsequently crystallized to a fine grained ceramic. Interest in these materials stems from their ease of formation and the excellent physical and mechanical properties exhibited by the final product.

This study of the ceramics formed from glasses in the Li_2O-SiO_2 system was undertaken in order to obtain understanding of both the mechanism of nucleation and crystallization and the effect of crystallization on the mechanical properties of the material.

It was found that the nucleation treatment given the samples greatly affected both the crystallization rate and the activation energy for crystallization. Analysis of the results through a modified form of the Johnson-Mehl-Avrami equation showed that it was the nucleation

activation energy which was reduced during the more effective nucleation treatments. Use of the JMA equation also showed that crystal growth occurred in the form of rods. This crystalline morphology was substantiated by micrographs showing a spherulitic growth habit.

Small angle x-ray scattering studies confirm the conclusions of other investigators that nucleation in this system can be due to the presence of a metastable phase.

It was shown that the dynamic elastic moduli of the glass-ceramics increases with the volume fraction of crystals and the coefficient of thermal expansion decreases with crystallization.

The fracture strength of the glass-ceramics at various percentages of crystallization was measured using the diametral compression test. It was shown that the samples which had undergone only a short nucleation treatment exhibited a maximum in strength at small volume fractions of crystals. Samples which underwent longer nucleation treatments exhibited a continual increase in strength at all volume fractions. The relative magnitude of strength enhancement was also shown to increase with duration of nucleation treatment.

It was demonstrated that the strengthening effect of the crystals was due to the fact that the flaw size in

the composite was controlled by the mean free path between the crystals. The decrease in strengthening at larger percentages of crystals was shown to be due to porosity in the composites. The porosity was concluded to be a result of stresses set up between the crystals and the glass during crystallization, causing localized crack formation.

CHAPTER I

INTRODUCTION

A glass-ceramic is defined as a material which is formed in the glassy state, and which is subsequently partially or wholly crystallized by means of a controlled series of heat treatments.

The first record of the production of a glass-ceramic comes to us from Reaumur (1739), who crystallized a number of glass bottles by heat treating them packed in sand. There was little interest in glass-ceramics because of their poor strength, however, until more than two centuries later when Stookey (1956) developed the process for producing Pyroceram.

It was then discovered that by choosing the glass composition carefully, and heat treating under appropriate conditions, it was possible to produce a very fine grained ceramic material, possessing an extremely low coefficient of thermal expansion, and having a strength which is excellent in comparison with the glass from which it was formed. In addition, it was found that much more complicated shapes could be formed in the glassy state and crystallized without deformation than could be produced by such processes as hot pressing or sintering.

For these reasons, many investigators have tried to determine the exact mechanism of crystallization in glasses, so that the production of desired properties could be optimized.

In general, it has been found that either the addition of a nucleating agent such as TiO_2, P_2O_5, or Pt, or phase separation in the glass is necessary to the formation of a fine grained glass-ceramic. Results have also shown that a two step crystallization treatment must be employed, the first portion at lower temperature to promote nucleation, followed by a crystal growth period at higher temperatures.

This work was undertaken in an effort to completely characterize the nucleation and growth processes in a simple glass system, and to determine the effect of several variables on these processes. It was also the purpose of this investigation to relate the mechanical properties of the glass-ceramic (fracture strength, modulus of elasticity, coefficient of thermal expansion) to the microstructure of the partially crystalline product.

The Li_2O-SiO_2 system was chosen, not only because of its simplicity, but also because it is the basis for more complicated commercial systems. In addition, crystal growth rates have been determined for some Li_2O-SiO_2 compositions, and the influence of a nucleating agent on growth kinetics has also been examined in this system.

The effect of phase separation in the glass, the addition of TiO_2 and various nucleation times on the crystallization kinetics and the number and size of the subsequent crystals formed in glasses in the Li_2O-SiO_2 system are reported. It is shown how the mechanical properties of the partially crystalline glass are related to the volume fraction and size of the crystals and thereby to the nucleation treatment.

CHAPTER II

KINETICS OF CRYSTALLIZATION

General Theory

In order to fully understand the role of nucleation and growth in the crystallization of glass, it is first necessary to understand the thermodynamic and kinetic theories upon which these nucleation and growth mechanisms are based.

Tammann (1925) showed that crystallization in glass consisted of two separate processes, nucleation of the new crystalline phase, and subsequent growth from these nuclei. Tammann found, however, that these two processes occurred at different temperatures, the maximum rates of nucleation and growth being several hundred degrees apart. In this review, the nucleation and growth steps will first be considered separately. It will then be shown how the kinetics of crystallization may be determined when nucleation and growth occurs simultaneously.

Nucleation

Classically, the nucleation of a crystalline phase in glass can be described by a change in free energy, ΔF.

If pressure and strain effects are neglected, and nucleation proceeds homogeneously, the relationship describing the free energy change as a clump of new phase is formed, is given by

$$\Delta F_r = 4/3 \Pi r^3 \Delta F_v + 4 \Pi r^2 \sigma \tag{1}$$

r - is the radius of the clump of new phase

σ - is the surface energy/unit area

ΔF_v - is the free energy/unit volume change during the transformation

The free energy change necessary to form a stable nucleus can be calculated by setting the first derivative of equation (1) equal to zero. One then obtains

$$\Delta F^* = \frac{16 \Pi \sigma^3}{3 (\Delta F_v)^2} \tag{2}$$

$$r^* = \frac{2\sigma}{\Delta F_v} \tag{3}$$

where ΔF^* is the critical free energy, and r^* is the critical size of the nucleus.

The rate of homogeneous nucleation may also be calculated using basic thermodynamic concepts. Again, strain energy is neglected, and σ is assumed to be isotropic. Two activation energies are involved in this case. They are ΔF^*, which has already been discussed, and ΔF_a, the

activation energy for an atom to cross the surface between the glass and the crystal, that is to disconnect itself from the glassy phase, and attach itself to the crystal.

If the formation and growth of nuclei of critical size is occurring, the nucleating rate can be given by the following expression

$$I = K_v \exp\left|\frac{\Delta F^* + \Delta F_a}{kT}\right| \qquad (4)$$

I is the nucleation rate, and K_v is a constant containing a number of pre-exponential terms including the frequency with which atoms are attached to the new surface.

In considering the variation of I with temperature, ΔF_a in equation (4) is fairly insensitive to temperature, but ΔF^* decreases fairly rapidly with supercooling [Fine (1964)]. K_v is only slightly temperature dependent in comparison to the exponential terms. At very large ΔT's the ΔF_a term predominates, and

$$I = \propto \exp\ (-\Delta F_a/kT)$$

Relationships similar to those shown above may be derived for the case in which nucleation occurs heterogeneously rather than homogeneously. Heterogeneous nucleation is the usual mode of transformation in glasses, where second phase particles may act as nucleation sites for the crystalline phase.

For the case of heterogeneous nucleation

$$\Delta F^{*} = \left|\frac{16\Pi\sigma^{3}_{\alpha\beta}}{3(\Delta F_{v})^{2}}\right|\left|\frac{2 - 3\ell + \ell^{3}}{4}\right| \qquad (5)$$

where $\ell = \cos\theta$, θ being the contact angle between the new phase and the substrate on which it is growing.

The rate of hetergeneous nucleation is given by a relationship similar to equation (4).

$$I = \sum_{j=0}^{j=\max} N_{j}/V\ K_{j}\ \exp\left|-\frac{\left(\Delta F^{*}_{j} + \Delta F_{a}\right)}{kT}\right| \qquad (6)$$

ΔF^{*}_{j} is the activation energy for nucleation on a particular site; ΔF_{a} is again the energy required to transfer a molecule from the glassy to the crystalline phase; N_{j}/V is the number of such sites per unit volume; K_{j} is the frequency factor for heterogeneous nucleation. There may be a distribution of sites, some more energetically favorable for nucleation than others. If an energy distribution is present, then a distribution in nuclei sizes should occur, since the more energetic sites will nucleate first.

Growth

Several theories have been proposed which describe the growth rate of second phase crystals in glass.

Turnbull (1956) and Turnbull and Cohen (1960) have made extensive contributions to the theory of nucleation and growth of crystals. He has developed an equation of the following form:

$$G = \frac{fkT}{3\Pi a_0^2 \eta} \left| 1 - \exp\left(\frac{\Delta F}{kT}\right) \right| \tag{7}$$

where f is the fraction of sites in the interface to which molecules can be attached; ΔF is the motivating free energy per molecule; a_0 is the jump distance; η is the viscosity in poises. Since

$$\Delta F = \frac{\Delta H_f \Delta T}{T_M}$$

and

$$kT >> \Delta F$$

then

$$G = \frac{f\Delta H_f}{3\Pi a_0^2 T_M} \frac{\Delta T}{\eta} \tag{8}$$

where

ΔH_f = enthalpy of crystallization

T_M = melting point of crystals

Hillig and Turnbull (1956) examined data on crystal growth in several materials. They found that the growth rate varied more rapidly than would have been expected from

equation (8). They found that the results were best described by the following empirical equation:

$$G = A/\eta(\Delta T)^{1.75} \tag{9}$$

where

A = constant and

η = viscosity

Frenkel (1946) has also derived equations describing the nucleation and growth of crystals. One such equation is the following:

$$G = A/\eta \exp - \frac{ZT_0}{T\Delta T} \tag{10}$$

T_0 is the equilibrium temperature; A and Z are constants.

All of the above equations have been applied to the growth of crystals in glass. Although a given equation may fit the experimental data fairly well for some cases, there does not appear to be a single fundamental equation which will describe crystal growth under all circumstances. Brown and Ginell (1962) have developed an equation which appears to fit any experimental data, but the equation, since it contains a number of adjustable constants, is strictly empirical.

Combined Nucleation and Growth

The kinetics of phase transformations may also be determined when nucleation and growth occur simultaneously. The treatment has been described by Burke and Turnbull (1952).

It is first assumed that G, the linear growth rate of an unimpinged crystal is independent of time. Then, if a particular crystal is nucleated at time t', then a linear dimension of the crystal at time t, where $t > t'$, will be given by $G(t-t')$. The volume of the crystal will be given by the following expression:

$$V_p = gG_xG_yG_z(t-t')^3 \tag{11}$$

where G_x, G_y, and G_z are the growth rates in the x, y, and z directions, and g is a shape factor.

The nucleation rate is given by:

$$I = \frac{dN_c}{dt} \tag{12}$$

Neglecting impingement, the total volume of new phase at time t in a volume V_0 of sample is:

$$V_t = \int_{t'=0}^{t'=t} V_p V_o dt'$$

dN_c

and

$$\frac{V_t}{V_o} = V_v = \int_{t'=0}^{t'=t} V_p dN_c \tag{13}$$

It is necessary to correct the above equation for the fact that as the amount of transformed phase increases, the volume of glass available for nucleation decreases. Johnson and Mehl (1939) made the correction by multiplying the expression under the integral in equation (13) by the fraction of glass untransformed, $(1 - V_v)$. Then

$$d(V_t/V_o) = dV_v = V_p(1 - V_v)dN_c$$

and

$$\ell n(1 - V_v) = - \int_{t'=0}^{t'=t} V_p dN_c$$

yielding

$$1 - V_v = \exp\left| - \int_{t'=0}^{t'=t} gG_xG_yG_z(t-t')^3 I dt' \right|$$

so

$$V_v = 1 - \exp\left| - \int_{t'=0}^{t'=t} gG_xG_yG_z(t-t')^3 I dt' \right| \tag{14}$$

Equation (14) describes phase transformations in a system in which crystal growth occurs in three dimensions. This equation can be generalized to the case in which growth may be occurring in only one or two dimensions. The equation then becomes:

$$V_v = 1 - \exp\left| - \int_{t'=0}^{t'=t} g\mathrm{I}G^n (t-t')^n dt' \right| \qquad (15)$$

As shown in equation (14), for three-dimensional growth, $G = G_x G_y G_z$, and n, an integer which depends on the dimensionality of the growth mechanism, is equal to three. However, n = 2 for two-dimensional growth, where $G = G_x G_y$, $G_z = 0$ (plates). For growth in only one dimension, n = 1, where $G = G_x$, $G_y = 0$, and $G_z = 0$ (rods).

$$V_v = 1 - \exp\left| - g^* \mathrm{I}G^n \ t^{n+1} \right| \qquad (16)$$

where

$$g^* = \frac{g}{n+1}$$

Equation (16) results from the integration of the expression in the exponent in equation (15). The nucleation rate, I, has been assumed to be independent of time, although Avrami (1941) showed that this assumption is not essential to solving the equation. Equation (17) was obtained from

(16) by taking the double logarithm of both sides of the equation

$$\ln\ln\left(\frac{1}{1-V_v}\right) = (n+1)\ \ln t + (n+1)\ \ln\ (g^{*}IG^{n}) \qquad (17)$$

If the temperature dependence of the nucleation and growth rates is included in equation (16), equation (18) results [DeHoff (1968)].

$$V_v = 1 - \exp - g^{*}t^{(n+1)}I_o e^{-Q_I/RT}\left(G_o e^{-Q_G/RT}\right)^{n} \qquad (18)$$

Q_I and Q_G represent the activation energies for nucleation and growth respectively. At constant V_v, one obtains equation (19) by rearranging the terms of equation (18) and taking the logarithm of both sides.

$$\ln t(V_v) = \frac{Q_I + nQ_G}{(n+1)\ R}\ \frac{1}{T} - \frac{\ln G_o^{n}I_o g^{*}/\ln\left(\frac{1}{1+V_v}\right)}{n+1} \qquad (19)$$

If the logarithm of the time to form a given volume fraction of crystalline phase is plotted against 1/T, the slope will be $Q_I + nQ_G/(n+1)R$. If V_v in equation (19) is taken to be 0.5, the above plots become the normal Arhennius plots usually made to determine the activation energy of crystallization. The measured activation energy for crystallization is then seen to be a combination of the activation energies for nucleation and growth. The results of the application of equation (19) to the data will be given later.

Previous Studies of Glass Crystallization

Crystallization in glasses usually proceeds heterogeneously rather than homogeneously, and can therefore be influenced by the addition of other components which can act as nucleation sites. It has been shown that the formation of collodial suspensions, phase separation, or the presence of metastable crystalline phases can aid nucleation of crystals in a glass. However, an understanding of the mechanisms involved in the behavior of heterogeneous agents is largely missing. Several investigations of these variables in the Li_2O-SiO_2 system have been conducted since it is the basis for many of the commercial glass-ceramics. This work includes the effect of nucleating agents such as Au, K, and Pt, the type and growth rate of the crystals which are formed, and measurement of the activation energy for crystal growth.

As mentioned previously, Reaumur (1739) first studied crystallization in glass more than 200 years ago. He heated glass bottles in sand for several hours or days. The result was a "porcelain" article which contained crystalline needles extending inward from the surface of the glass. We now know that this type of crystallization which produced a weak and brittle structure occurs because of the lack of nucleation within the bulk of the glass.

All crystallization then takes place at the surface of the article.

Nucleation can be promoted in glass by a variety of methods. Historically, one of the first ways in which glass has been nucleated is through the precipitation of metallic colloids, Hench (1967). Copper, silver, gold, or any of the platinum group metals are frequently used for this purpose. When glass containing these metals is heated, colloidal size particles are formed and the glass becomes colored. It appears that the metal crystals must grow to a size of about 80 Å to be effective nucleating sites, Fletcher (1958).

Precise control over the nucleation by metallic particles can be obtained through a process termed photonucleation, Stookey and Maurer (1962). The reduction of the metallic ions is accomplished through the use of ultraviolet light or x-rays.

Phase separation in glasses is also a possible means of nucleation. From equation (5) in the previous section, it is seen that the free energy of formation of a nucleus is lowered by the reduction of surface energy associated with the presence of a droplet. Ohlberg, Golob, and Strickler (1962) studied the crystallization behavior of three multi-component glasses. They concluded that the surface of droplets resulting from a glass in

glass separation acted as the nucleating agents in these glasses. They found that growth could proceed first into the droplet, and from there into the matrix, or could grow directly into the matrix, leaving the droplet uncrystallized.

It has also been shown that the addition of small quantities of compounds such as TiO_2 or P_2O_5 may promote phase separation at compositions in glass systems where this phenomenon does not normally occur. Stookey (1956) discovered that certain glasses containing small amounts of TiO_2 could be crystallized to fine grained, high strength ceramics. He suggested that the addition of TiO_2 to glasses promotes the formation of isotropic regions ("emulsions") which are unstable to crystallization. Vogel and Gerth (1962) have studied several systems which crystallize in this manner, and theorize that the surface of these droplets act as the nucleating agent. Phillips and McMillan (1965) have found that the addition of P_2O_5 to glass produces a similar behavior.

Work recently completed indicates that the addition of larger amounts of TiO_2 may produce a different effect. Nakagawa and Izumitani (1968) showed that when 22 w/o TiO_2 was added to a Li_2O-SiO_2 glass that crystals of Li_2O-TiO_2 which formed during heat treatment acted as the nucleating agents in the glass.

Other investigators have demonstrated the possibility that metastable crystalline phases may be precursors to the final stable crystalline phase. Ruiz-Menacho and Roy (1959) showed that in the system Li_2O-Al_2O_3-SiO_2, a very high silica phase formed and then reacted with the remaining environment to give the equilibrium phases. Welch (1956) noted the metastable crystallization of corundum at the anorthite composition near the liquidus in the MgO-Al_2O_3-SiO_2 system. It was concluded by Roy (1962) that a metastable transitory phase is not only possible, but very likely to occur during the glass crystallization process.

The physical and mechanical properties of a Li_2O-ZnO-SiO_2 glass-ceramic were measured by McMillan, Phillips, and Partridge (1966). By using differential thermal analysis they found an exothermic peak at 550°C. Although they had no clear evidence of its existence, the authors predicted the crystallization of lithium metasilicate (Li_2SiO_3) at this temperature. They postulated that this phase formed and then dissolved as crystallization proceeded.

Because of the compositional complexity of commercial systems, several investigators have examined the Li_2O-SiO_2 binary system in an attempt to understand the basic nucleation and growth mechanisms.

Differential thermal analysis and optical microscopy were employed by Matveev and Velya (1960) to study crystallization in a series of compositions in this system. The authors found that the crystallization of $Li_2Si_2O_5$ begins about 600 ± 20°C as shown by an exothermic DTA peak at this point. This temperature was found to be essentially unchanged as the composition of the glass was shifted from Li_2O-$2SiO_2$ to Li_2O-$6SiO_2$. It was also discovered that most of the $Li_2Si_2O_5$ phase crystallized as spherulites. In many cases the centers of the spherulites contained a monolithic mass of crystals which were surrounded by the radial crystals usually associated with spherulitic growth. It was proposed that the centers grow from the glass matrix until diffusion is impeded, at which time radial growth then becomes the most efficient means of crystallization.

The effect of K and Au additions on the crystallization of $Li_2Si_2O_5$ from glass of the same composition was investigated by Matsuda and Suito (1964). They determined the kinetics of crystallization in a glass sample which had been crushed to a size such that it would pass through a 300 mesh screen. Under these conditions, the surface of the glass particles would act as nucleating agents for the crystals of $Li_2Si_2O_5$. An activation energy of growth of the crystals of 49 Kcal/mole

was measured. It is interesting to note that when Au and K were added to the glass composition, Li_2SiO_3 rather than $Li_2Si_2O_5$ was crystallized. This phenomenon was explained on the basis of the formation of a colloidal suspension, whose surface structure was favorable to the formation of Li_2SiO_3.

Degen and Toropov (1966) measured by optical microscopy the rate of radial growth of spherulitic needles at various temperatures in a glass of composition Li_2O-$2SiO_2$. They found that the radial growth rate was constant with time at a given temperature, and determined an activation energy for growth of 49 Kcal/mole. Since the activation energies for lithium and oxygen ion diffusion in glass of this same composition are 19.1 Kcal/mole and 32.4 Kcal/mole respectively (Kuznetsov (1959) and Douglas and Mohyuddin (1960)), Degen and Toropov proposed that the diffusion of lithium-oxygen ion complexes was the rate controlling step in the growth process.

Jaccodine (1961) studied the growth rates of $Li_2Si_2O_5$ crystals in a 30 mole % Li_2O glass by means of the optical microscopy of polished sections. He measured an activation energy for growth of approximately 49 Kcal/mole.

The effect of temperature on crystalline growth rates at several compositions in the Li_2O-SiO_2 systems was

measured by Morley (1965) by means of high temperature optical microscopy. An average activation energy of approximately 56 Kcal/mole can be calculated from the plots of his data. Morley attempted to fit his growth rate versus temperature data with one of the growth equations discussed in a previous section. He found that the theory proposed by Frenkel (equation 10) gave the best agreement with the experimental results, but that Hillig's equation (9) also fit fairly well.

Rindone (1962) investigated the effect of platinum additions on the rate of crystallization of $Li_2Si_2O_5$ from a glass of composition Li_2O-$4SiO_2$. The per cent of crystallinity was measured by quantitative analysis of the x-ray diffraction peaks of $Li_2Si_2O_5$. The kinetics and an activation energy of crystallization were determined for additions of platinum from 0 to .01%. The results of Rindone's work are summarized in Table 1 below.

TABLE 1

VARIATION OF ACTIVATION ENERGY OF CRYSTALLIZATION WITH ADDITION OF Pt (after Rindone)

% Pt × 10^3	Q Kcal/mole
0	120
1	95
5	50
10	60

It was Rindone's opinion that the size of the platinum nuclei was paramount in determining their effectiveness as nucleating agents. It is his contention that the platinum nucleus surrounds itself with lithia rich clusters which subsequently crystallize. When the platinum nucleus becomes too large, its surface free energy decreases so that there is less tendency for it to surround itself with lithia, and its nucleating effect is decreased.

Rindone (1962) also found that the $Li_2Si_2O_5$ crystals which form on the surface of a devitrified sample show a preferred orientation, with the (002) plane parallel to the glass surface. The preferred orientation of the crystals persists to great depths in non-nucleated glasses. When platinum was added to the glass the preferred orientation was reduced considerably.

These results establish the fact that the nucleation of crystals in glasses may be influenced by many variables. It is apparent, however, that there are considerable differences of opinion as to what is the relative importance of phase separation or metastable phase in promoting nucleation in glasses.

In the Li_2O-SiO_2 system it has been shown that crystallization is affected by addition of elements such as Pt, K, or Au, that crystal growth is primarily

spherulitic in nature, that the crystal growth rate is constant, and that the activation energy for growth is approximately 49 Kcal/mole.

It will be shown in this work in what manner both nucleation and growth of crystals in the Li_2O-SiO_2 system are affected by several of the above conditions, and a mechanism of nucleation and growth will be proposed.

CHAPTER III

MECHANICAL PROPERTIES OF GLASS-CERAMICS

It will be shown that for several glass systems, the fracture strength of the crystallized ceramic is considerably greater than the strength of the parent glass. The effect of the ceramic grain size and therefore the nucleation treatment is shown to play an important part in determining the strength. In other systems, the strength of the material is shown to decrease with crystallization, probably due to stresses occurring around the anisotropic crystals.

The investigation of a number of model glass-particle systems has led to several theories as to the effect of crystals as a strengthening medium in the glass.

Strength of Glass

A measurement of the force necessary to completely separate two neighboring atoms in a glass leads to the calculation of a theoretical strength of 3 to 4 million psi.

This value is very surprising since most bulk glasses exhibit a strength in the range of 5000 to 15,000 psi. The solution by Inglis (1913) of the notch problem in engineering materials was a major step in relating

practical failure-stress to theoretical strength. The conclusion was reached that irregularities or flaws within the bulk or on the surface of specimens acted to concentrate applied stresses to values which would locally exceed the theoretical strength of the material, and permit crack propagation to occur. The equation developed by Inglis is given below:

$$\frac{\sigma_m}{\sigma_a} = \sqrt{c/\rho} \tag{20}$$

where

σ_m = concentrated stress at crack tip

σ_a = applied stress

c = crack depth

ρ = curvature of crack tip

Griffith (1921) later put forward his well-known relationship that established the conditions that would lead to instability of a crack or flaw in an elastic medium. By equating the energy of elastic deformation in the region of a crack to the energy required to form new surface, it could be predicted, that for a given flaw geometry, an applied stress in excess of a critical value would lead to spontaneous crack propagation. The Griffith relationship is given by:

$$\sigma_{cr} = \sqrt{4E\gamma/\pi c} \quad (21)$$

where

σ_{cr} = applied failure stress

E = Young's modulus

γ = surface energy

c = crack length

Another important facet of the explanation of the strength of glass is the statistical nature of the fracture process. All of the statistical theories are based on the contention that "a chain is only as strong as its weakest link." Their common mathematical basis is shown below.

Let the underlying probability distribution of flaw strengths s be $f(s)$, so that the probability that the strength of a given flaw lying between s_1 and s_2 is:

$$\int_{s_1}^{s_2} f(s)\,ds$$

The probability that the strength of a given flaw is less than s is:

$$F(s) = \int_{-\infty}^{s} f(s)\,ds$$

For a sample containing n flaws, the cumulative strength distribution function is:

$$G_n(s) = \int_{-\infty}^{s} g_n(s)\,ds = 1 - \left|1 - F^{(s)}\right|^n$$

Most statistical theories differ from one another only in the form of the distribution function $f(s)$.

One consequence of this statistical nature of glass failure is the fact that the strength of glass samples increases as the size of the sample decreases.

Another important aspect of the strength of glass is its dependence on both atmosphere and loading rate during testing. Many investigators such as Preston, Baker, and Glathart (1946), Gurney and Pearson (1952), Shand (1954), Charles (1958), and Mould and Southwick (1959) have reported on the effect of delayed failure in glasses. Delayed failure appears as a reduction in the measured strength of glass as the time of loading is increased. However, the extent of this reduction is sensitive to both temperature and atmosphere. Testing in vacuum reduces the weakening effect of increased loading time but does not eliminate it. If, however, strength tests are conducted at temperatures below about 120°K, all effects of loading rate are eliminated. The principal explanation for the phenomena of delayed failure has been proposed to be a tensile stress modified reaction between glass and water vapor at the tips of surface cracks. This reaction

is also thermally activated, probably being controlled by alkali ion diffusion in the glass.

Previous Studies of Mechanical Properties of Glass-Ceramics

Several investigators have reported on the effect of crystallization on the mechanical properties of a glass-ceramic. Most of these investigations, however, have been concerned only with the properties of the fully crystalline product and not with the properties at intermediate stages of crystallization.

McMillan (1964) discusses some of the results obtained by Stookey (1959) for the modulus of rupture of various glass ceramics. Stookey found that the average strength of a number of TiO_2 nucleated glass-ceramics was 17,000 psi.

This value should be compared with the moduli of rupture of bulk glasses which rarely exceed 10,000 psi.

McMillan also discusses the effect that different crystalline phases in the same system may have on the strength of a glass-ceramic. The interesting feature revealed by the data is that while compositions which contain beta-spodumene as a major phase have cross-breaking strengths of 18,000 to 20,000 psi, those containing beta-eucryptite have strengths in the range of 10,000 to 11,000 psi. McMillan proposes that the lower strength may be

connected with the extremely low thermal expansion coefficient of beta-eucryptite so that the local stresses in these glass-ceramics may be higher than those in materials containing beta-spodumene.

McMillan also proposes that the very small grain size in glass-ceramics plays one of the most important parts in determining its increased mechanical strength. It is his opinion that one of the reasons for the dependence of strength on grain size is the existence of boundary stresses between adjacent crystalline or vitreous phases. These can be generated as the result of differential thermal contraction of the phases or can arise due to the presence of a phase having anisotropic expansion properties. The boundary stresses, which in some cases can cause cracking between grains, are minimized by small crystal sizes.

Watanabe, Caporali, and Mould ([illegible]) measured the flexure strength of a heterogeneously nucleated glass in the system Li_2O—Al_2O_3—K_2O—SiO_2 for both unabraded and grit blasted specimens in the glassy state and after various stages of heat treatment. The strength of abraded specimens increased during crystallization from 11,000 to 27,000 psi, while the strength of the pristine samples decreased from 80,000 to 38,000 psi. The material was shown to exhibit static fatigue in all stages of heat treatment.

No attempt was made, however, to determine percentage or sizes of crystals developed in the glass-ceramics during heat treatment.

It was shown by Tashiro, Sakka, and Wada (1960) that the strength of a Li_2O-K_2O-Al_2O_3—SiO_2 glass-ceramic was dependent on the amount of platinum added as a nucleating agent. These investigators found that the bending strength increased from 11,600 to 36,000 psi as the amount of platinum was increased from 0 to 0.1%. The effect of the platinum was apparently to decrease the crystal size in the material.

The effect of crystallite size on the strength of a multi-component glass-ceramic was studied by Tashiro (1966). He found an inverse square root relationship between strength and crystal length.

Ownby (1962) studied the strength and microstructure of a Li_2O-Al_2O_3-MgO-SiO_2 glass-ceramic. He measured the fracture strength after various heat treatments, using the diametral compression test. He found that the strength increased initially with heat treatment, but then decreased. The strength of the completely crystallized glass-ceramic material was found to be dependent on the initial nucleation period.

The effect of per cent crystallization on the transverse strength of a multi-component glass was measured

by Davis (1966). He found that both diopside ($CaO \cdot MgO \cdot 2SiO_2$) and beta-eucryptite ($Li_2O \cdot Al_2O_3 \cdot 2SiO_2$) crystallized from the glass. The ratio of these two phases varied with amount of crystallization. The strength of both abraded and unabraded rods was found to decrease as the percentage of crystals increased. The cause for this decrease was proposed to be flaws initiated at the crystal boundaries due to the large difference in thermal expansion between the crystals (especially beta-eucryptite) and the glassy matrix.

Although the effect of volume fraction and size of crystals devitrified from a glass has not been investigated until now, model systems of crystals and glass fabricated by vacuum hot compaction have been studied.

Model Glass-Particle Systems

In order to measure independently the many variables which may affect the strength of glass-ceramics, investigators have studied several glasses to which were added a given volume fraction of particles of a known size and shape. These composites were usually made by hot pressing the particles and glass.

Fulrath (1959) determined internal stresses in various glass-alumina compacts by measuring x-ray peak shifts. A marked increase in internal strain was found as the crystal particle size was decreased from 400 to

less than 8 microns. Fulrath also found that if the particle size was kept constant, the strength of the compacts decreased with increasing internal strains.

Grossman (1961) applied the same techniques to thoria-glass compacts.

Strength trends in mullite-glass compacts were explained by Studt and Fulrath (1962) on the basis of interfacial chemical reactions.

The mechanical strength of alumina-glass and zircon-glass compacts was investigated by Binns (1962) as a function of internal stresses. The results showed a maximum in strength at particle volume fractions of approximately 0.4.

Jacobson (1962) substituted nickel spheres, 37 to 44 microns in diameter, as a dispersed crystalline phase in two different glass compositions. He found that if the matrix was a glass having a smaller thermal expansion coefficient than the nickel, there was a decrease in strength for all volume fractions of Ni particles, but if the matrix had a larger thermal expansion coefficient than the nickel, the modulus of rupture increased from about 5500 to 11,500 psi as the volume fraction of Ni particles was increased from 0 to 0.5. This difference can be attributed to the fact that in the latter system the

non-reactive Ni particles were clamped in place by the glass, while in the first system they were not.

Nason (1963) compacted tungsten and nickel particles of various sizes in a soda-borate glassy matrix. The moduli of rupture of these compacts were measured for varying volume fractions of particles. In general, it was found that the strength of the compacts containing tungsten spheres increased with volume fraction of spheres. The increase was independent of whether the coefficient of thermal expansion of the glass was greater or less than that of the tungsten. This result seemed to indicate that boundary stresses surrounding the particles were not important.

When nickel spheres were substituted for the tungsten, a decrease in strength occurred for all volume fractions. This decrease was attributed to a lack of bonding between the nickel and the glass, in contrast to the tungsten which was strongly bonded to the matrix.

An equation which predicted the stresses around a second phase particle due to differences in thermal expansion coefficient was developed by Selsing (1961). This equation is given below.

In the glass:

$$p_r = - 2p_t = - PR^3/r^3 \qquad (22)$$

where

p_r = stress in the radial direction

p_t = stress in the tangential direction

R = radius of the particle

r = distance from the center of the particle

P = pressure on the particle due to thermal expansion coefficient differences

In the particle:

$$P_r = P_t = - P \tag{23}$$

where

$$P = \frac{(\alpha_g - \alpha_p)\ \Delta T}{\frac{1 + \nu_g}{2E_g} + \frac{1 - 2\nu_p}{E_p}} \tag{24}$$

where

α = thermal expansion coefficient

ν = Poisson's ratio

E = Young's modulus

The subscript g refers to the glassy matrix; p refers to the particle.

Nason (1963) and Frey and Mackenzie (1967) used Selsing's expression to calculate the stresses which occurred in several glass-particle compacts.

Hasselman and Fulrath (1966) proposed a theory to explain fracture in a glass-particle composite. They divided the effect of the crystalline dispersions into two regions. In region I the average distance between particles is greater than the flaw size. At least on a statistical basis, however, the average flaw length will be reduced in proportion to the volume fraction of dispersed phase, as:

$$c = c_o(1 - V_v) \tag{25}$$

where

c = flaw size in the composite

c_o = original flaw size in the glass

V_v = volume fraction of the dispersed phase

Substituting for a in Griffith's (1921) equation:

$$S_o = \left(\frac{4\gamma E}{\Pi c}\right)^{1/2} \tag{26}$$

where

γ = surface energy of the glass

E = Young's modulus

one obtains:

$$S = S_o(1 - V_v)^{1/2} \tag{27}$$

It is seen that theoretically there should be an increase in

strength of glass-crystal composites even at very low volume fractions of crystals.

In region 11, at higher volume fractions or smaller particle sizes, the flaws will be larger than the average distance between particles, i.e. flaw size is now governed by the mean free path between particles. An expression for mean free path, λ, between spherical particles of uniform radius, R, can be obtained from the expressions given by Fullman (1953). This expression is:

$$\lambda = \frac{4R(1 - V_v)}{3V_v} \tag{28}$$

Substituting λ for c in equation (26) yields for the strength in region 11.

$$S = \left| \frac{3\gamma E V_v}{\Pi R(1 - V_v)} \right| \tag{29}$$

Hasselman and Fulrath showed, that for a dispersion of various particle sizes of Al_2O_3 in a sodium borate glass having the same thermal expansion coefficient as the Al_2O_3 crystals, that bending strength varied directly as the inverse square root of the mean free path between the particles when the mean free path was larger than 40 µ. Below this value (Region 1) the strength was nearly constant with mean free path.

It was shown by Frey and Mackenzie (1967) that the strength of several Al_2O_3 and ZrO_2 glass composites increased even in the volume fraction range which Hasselman and Fulrath designated Region 1. They also found that some composites, in which the stresses due to differences in thermal expansion coefficient between the matrix glass and the particles were excessively large, did not show a strength increase upon addition of Al_2O_3 or ZrO_2. This lack of strengthening was attributed to cracks being present in the glassy matrix before flexure strength tests were performed. Frey and Mackenzie proposed that, in general, the strengthening of the Al_2O_3 and ZrO_2 inclusions was due to the increased elastic properties of the composites rather than to the restriction of flaws.

Hasselman and Fulrath (1967) also investigated the effect of micromechanical stress concentrations on the strength of two phase brittle-matrix ceramic systems. The dispersions, whose elastic properties differed from that of the glassy matrix, consisted of 60 μ alumina particles and pores, 60 μ in diameter. They calculated the effect of the pores and particles under both uniaxial and biaxial loading. They used the solutions of Goodier (1933) for stress concentrations around a circular inclusion in a flat plate to calculate the micromechanical stresses in the systems. These solutions were used because it was felt

that they best represented the case of flaws in the surface of the sample, where fracture began.

From these equations it was calculated that tensile stresses greater than the applied stress by a factor of 1.4 may occur at the glass-particle boundary in this system. The authors' experimental results showed a precipitous decrease in strength with addition of porosity for both uniaxial and biaxial loading. In the case of biaxial loading of the glass-alumina composite, the strength was described by the following expression.

$$S = \frac{S_o}{K} (1 - V_v)^{1/2} \tag{30}$$

where K is a stress concentration factor which depends on the elastic properties of both phases.

It can be concluded from the above study that stress concentration effects can be significant in the determination of the strength of glass-particle systems if the difference in elastic properties of the two phases is large.

It is seen, therefore, that there are a number of variables which may influence the strength of glass-particle composites.

Fulrath, Grossman, and Binns showed that the presence of internal stresses may decrease the strength

of compacts. It was demonstrated by Nason, Studt, and Jacobson that chemical reactions at the glass-particle interface could influence the strength. The effect of the change in elastic modulus on the strength of composites was shown by Frey and Mackenzie. Hasselman and Fulrath showed that decreasing the mean free path between second phase particles would cause an increase in strength. They also pointed out that differences in the elastic properties of the glass and crystals would produce stress concentration which would be deleterious to the strength.

The theoretical analyses obtained from these model glass-particle systems will be used to explain the experimentally measured strength dependencies of partially crystalline glass-ceramics investigated in this program.

CHAPTER IV

EXPERIMENTAL PROCEDURE

Glass Composition

The primary constituents of the glasses used in this experiment consisted of 5 micron silica, reagent grade lithium carbonate, and reagent grade titanium dioxide. A complete chemical analysis of these raw materials is presented in Table 2. The constituents were weighed out in batches of approximately 400 grams on a Harvard trip balance. The accuracy in weighing was about ± .1 gram. The weighed batch was mixed thoroughly in a rotating jar mill without balls for approximately 1 hour.

Melting

The glass was prepared from the batch by first placing the mixture in a 150 gram platinum crucible and covering it with a platinum lid. Melting was carried out in a refractory furnace heated by electrically resistant SiC Glo-bars. Two melting temperatures were employed. Glass of the 33.3 mole % Li_2O composition and the 30 mole % composition was melted at 1350°C. Glass of the 26.4 mole % Li_2O composition was melted at 1420°C. These

TABLE 2

ANALYSIS OF GLASS RAW MATERIALS

Compound	Weight %
Lithium Carbonate[1]	
Li_2Co_3	99.3
Na_2Co_3	0.2
Iron	.0008
Sulfate	0.3
Chloride	.0003
Calcium	.0003
Phosphate	.0001
Silicon Dioxide[2]	
SiO_2	99.91
Iron	.019
Alumina	.08
Titania	.009
Calcium and Magnesium	Trace

[1]Foote Mineral Company.

[2]Pennsylvania Glass Sand Company.

compositions are shown on the phase diagram presented in Figure 1. A study was carried out to determine whether there was an effect of melting time on the subsequent structure and properties of the glass.

Electron micrographs taken from replicas of etched fracture surface of the glass poured after times ranging from 18 to 54 hours showed no detectable structural differences. All of the glass used in these experiments was held at temperature for times within this range. No differences in results obtained from different batches of glass could be noted. Some samples were analyzed for the presence of platinum on an emission spectograph, but no traces of platinum were detected.

Casting

The glass used for the kinetics of crystallization investigation and for the study of the mechanical properties of the partially crystalline glass-ceramic was cast into a mild steel mold in which a 13 mm diameter, 25 mm long hole had been reamed and then smoothed using 600 grit SiC paper. The mold rested on a smooth steel plate. The top of the mold was open, and no plunger was used to quench the top of the glass sample after pouring. The samples employed in the electrical and x-ray small angle scattering measurements were cast into a steel mold, 17.5 mm in diameter.

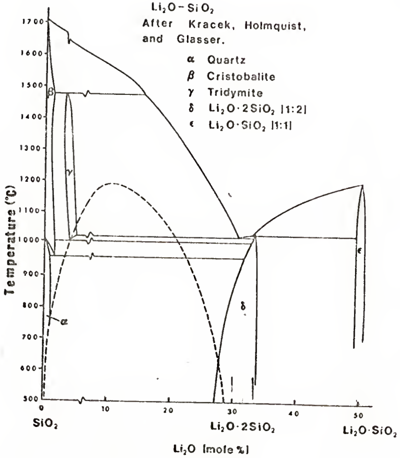

Figure 1.--Phase diagram of the Li_2O-SiO_2 system.

A plunger was pressed into the molten glass in order to produce flat specimens from 3 to 8 mm thick. In all cases, the crucible was returned to the furnace after each specimen was cast, and the remaining glass was allowed to reach the melting temperature before the next sample was poured.

All specimens except those of the 26.4 mole % composition were clear. The as cast 26.4 mole % glass was bluish, indicating that phase separation had already occurred. The existence of phase separation in this glass is substantiated in the electron micrograph presented in Figure 2. The droplets are SiO_2 rich; the matrix is Li_2O rich.

After they were cast, all specimes were heat treated at 300°C for one hour in order to reduce the stresses in the sample to a level at which sudden breakage would not occur. Even after this heat treatment, stresses as high as 4000 psi could be detected in some samples by the measurement of stress birefringence.

Heat Treatment

The crystallization of all of the glass used in this series of experiments was carried out in two steps, a nucleation heat treatment for various times at 475°C, followed by a heat treatment at temperatures between 549° and 610°C, during which crystal growth occurred. All heat

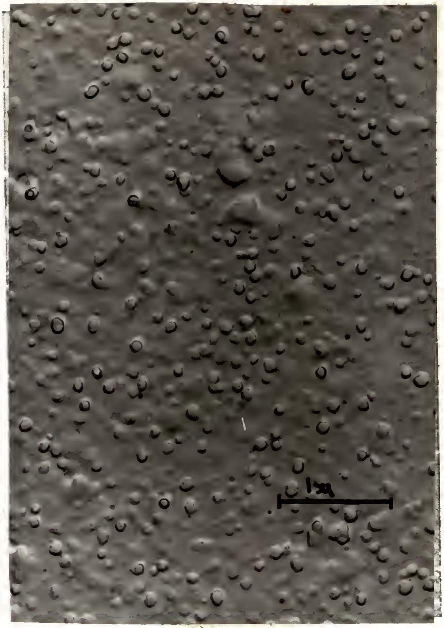

Figure 2.--Phase separation in an as cast 26.4 mole % glass.

treatments were made in a nichrome wound tube furnace containing a high purity aluminum block. The thermal gradient in the furnace was 1°C in two inches within the aluminum block. The samples reached the set temperature approximately 25 minutes after they were placed in the furnace.

It was found that the nucleation treatment was necessary in order to promote homogeneous bulk crystallization within the glass. Otherwise a large amount of surface crystallization occurred, and crystallization within the sample itself was very non-homogeneous. The effect of several nucleation times on the subsequent crystallization behavior was also investigated.

Experimental Analysis

Kinetics of Crystallization

The samples used for the study of the kinetics of crystallization were crystallized to various volume fractions of crystals after being given a nucleation treatment. After the crystallization treatment the samples were prepared for x-ray analysis by breaking them into small pieces, and grinding the pieces in a shaker mill. The samples were held in the mill in a capsule provided with tungsten carbide ends, and containing a ball of the same material. After rough grinding in the mill,

the samples were further ground in an alumina mortar and pestle until they passed through a 200 mesh Tyler screen. X-ray diffractometer specimens were then prepared according to the method of Munch and Pierron (1963). The first part of this method consists in weighing out a quantity of the powdered sample on an analytical balance. Although the same weight of sample (approximately .2 grams) was used each time, it was seen that this weight was not critical to the accurate determination of the per cent crystallinity. The weighed sample is mixed with di-octyl phthalate which forms a slurry with the powder. A glass slide is prepared by placing strips of 7 mil thick electrical tape across each end. The slurry is spread on the slide, and smoothed until it is the same thickness as the tape. This means that when the slide is inserted into the x-ray diffractometer, the top of the sample is in the correct plane for diffraction.

Samples prepared as described in the previous paragraphs were analyzed for per cent crystallinity on a Norelco x-ray diffractometer, using Cu $K\alpha$ radiation. The diffractometer was equipped with a curved crystal monochromator which reduced background effects. The diffractometer goniometer was operated at a speed of 1°/min from 11° to 50° 2θ. The x-ray tube was operated at 40 KV and 15 ma.

Before any unknown samples were analyzed, a set of standard samples containing known volume fractions of $Li_2Si_2O_5$ crystals were analyzed with the diffractometer. The results are shown in Figure 3.

The abscissa on this plot represents the percentage of crystallized material that was inserted into the standard samples. The ordinant is the ratio of the total peak heights of all of the x-ray diffraction peaks in the sample to the total peak height in a 100% crystalline sample. It was necessary to measure all of the peaks, since in this way the effect of preferred orientation is eliminated. It is seen that there is a one to one correspondence between relative peak height and per cent crystallinity, indicating that matrix effects in the sample are negligible. The error in determining per cent crystallinity in this manner is about ± 5%. It was also noted that the measurements could be repeated very accurately even after the sample was removed from the diffractometer and reinserted.

Fracture Strength

The samples which were to be used to measure the fracture strength of the glass-ceramic using the diametral compression test were cut from the center portion of the nucleated glass samples. Approximately 5/8 inch long

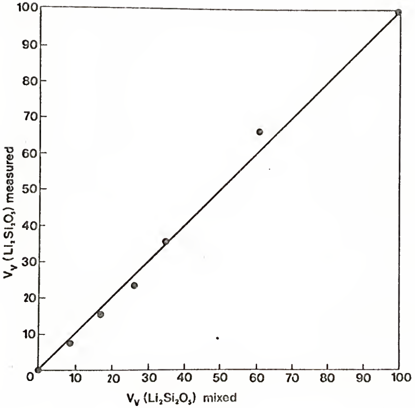

Figure 3.--X-ray determination of per cent crystallinity in standard samples.

sections were cut from the glass on a carborundum cut off wheel. These sections were then subjected to a heat treatment in order to produce a predetermined percentage of crystals. After the desired volume fraction had been attained, the samples were removed from the crystallization furnace and air cooled. They were then annealed at 440°C for 20 minutes in a separate furnace and furnace cooled at about 1/2° per minute in order to relieve any stresses that may have occurred during the crystallization treatment. It must be realized of course that the stresses due to the difference in thermal expansion coefficient between the crystals and the glass are still present after annealing. The annealing temperature was chosen by determining the thermal expansion characteristics of the glass, and choosing a temperature just below the transformation temperature for this composition.

The cylindrical sections were then polished using a special polishing rig designed to insure that the ends were parallel. The rig consisted of an aluminum disk, 8" in diameter, 1" thick in the center and 7/16" thick on the edge and was designed so that the edges of the disk rested on the edge of an 8" polishing wheel and the bottom of the disk extended to within 1/32" of the polishing paper. Five holes extending from the center to the periphery were drilled through the disk. The holes were machined so that

the samples would slip into them freely but would not tip while they were being polished. Brass plungers fitted into the top of the holes allowed pressure to be placed on the samples during polishing. Using this apparatus, it was possible to polish through 120, 180, 320, and 600 grit SiC papers while maintaining the parallelness of the sample ends within 2 mils. The samples were then polished by hand using .3 micron Al_2O_3 on Buehler microcloth.

The condition of the cylindrical surface of the samples was not altered.

The polished samples were kept in a desiccator until they were tested.

The diametral compression test was developed by Caniero (1947) as a test for the fracture strength of concrete. Wright (1955) used the technique in testing concrete cylinders and published his results with a review of the theory and a comparison with other strength tests. Berenbaum and Brodie (1958) also compared results obtained from the diametral compression test with other strength tests on plaster of Paris. They found that strengths measured by the diametral test were approximately 80% of those found by using a conventional tensile test. However, the diametral test yielded strengths only about 40% of those measured in a modulus of rupture test. Rudnick *et al.* (1963) have recently extended the theory to include other

ceramic materials. The test has been used on porcelain white wares [Moore (1962)] and glass [Kenny (1957)].

The test involves applying a compressive load along the diameter of a relatively short cylinder. The test was carried out on a 12,000 pound capacity U-Celtronic Tinius Olsen compression testing machine. Three-eights inch width strips of construction paper, 0.012 inches thick, were placed between the specimens and the loading platens. One reason for the use of loading pads is the fact that they tend to even out stress variations due to any irregularities in the sample surface. They also distribute the applied load over a band rather than a line so that the compressive stress at the sample surface is reduced, thereby reducing the chances of crushing at this point. The load distribution with the use of loading pads is presented in Figure 4. It can be seen that the tensile stress is nearly constant over three-quarters of the vertical plane, but reverses to a high compressive stress at each end. Although the maximum compressive stress is about 18 times the maximum tensile stress, the relatively low tensile strength of ceramics causes failure to always occur in tension.

The expression relating applied load to fracture strength for this test is given by equation (31).

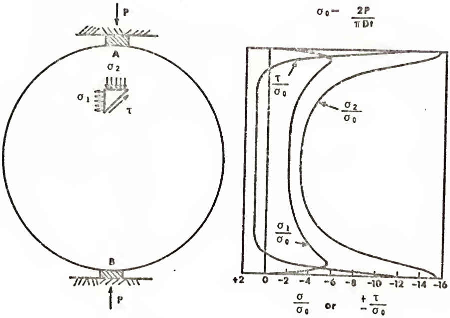

Figure 4.--Stress distribution across loaded diameter for a cylinder compressed between loading pads.

$$\sigma = \frac{2P}{\Pi D t} \tag{31}$$

where

P = applied load

D = diameter of specimen

t = length of specimen

The loading rate was kept constant at .2 in/min during this test. This meant that the effect of static fatigue, which is always present in the testing of glass, could be ignored. All of the tests were conducted in atmosphere at room temperature.

Results obtained by varying the above factors are presented in Appendix 1.

Thermal Expansion Coefficient

Samples to be used in measuring the coefficient of thermal expansion of the partially crystallized glass were prepared by casting glass rods 2" in length and 1/2" in diameter. These rods were cut and polished to 2" ± .05", and were then nucleated and heat treated to varying percentages of crystallization.

The thermal expansion coefficient was measured on an Orton Automatic Recording Dilatometer. The temperature of the sample was increased from 25°C to 300°C at a rate of nominally 2°/min.

Elastic Modulus

Specimens which could be used in the measurement of dynamic modulus were cut from 2" long rods of the nucleated glass. Sections about .1 in by .02 in were cut from these rods on a carborundum wheel. These sections were rough ground and polished on 180 grit SiC until all of the sides were parallel within ± 4 mils. These specimens were heat treated to various volume fractions of crystals.

The dynamic modulus of the partially crystalline specimens was determined by measuring the resonant frequency at which the bars vibrated. The apparatus consisted of a Brüel and Kjar Type 1022 Bent frequency oscillator coupled with a Type 2603 Microphone Amplifier and a Type 3930 complex modulus apparatus. The specimens were clamped at one end and driven in a flexural mode of vibration. The driver and pickup consisted of magnetic transducers. Small pieces of razor blade were glued to the specimens so that they would respond to the magnetic fluctuations.

The expression relating resonant frequency to the elastic modulus, given by Fine (1952), is presented in equation (32) below.

$$\sqrt{E/\rho} = f_n \frac{4\sqrt{3}\,\ell^3}{\Pi t \beta_n^2} \tag{32}$$

where

E = Young's modulus

ρ = density

ℓ = free length of bar

t = thickness of bar in direction of vibration

β_n = constant = 0.599 for the fundamental mode

Only the fundamental resonant frequency was measured because the amplitude of the higher modes were too small to be determined accurately.

The specimen was removed and replaced a number of times at each point, and the average of these measurements was taken.

Electrical Properties

The electrical properties of the heat treated glass were determined on 17.5 mm diameter disks, polished through 600 grit SiC paper. Double guard ring gold electrodes were plated onto the samples in an evaporator. The equipment and method of analysis described by Kinser and Hench (1968) were used to measure the electrical properties of the samples.

X-ray Small Angle Scattering

X-ray small angle scattering specimens were prepared from samples on which the electrical properties had already been measured. This was accomplished by attaching the

glass disk to a substrate with "Lakeside cement," and polishing the sample on 180 grit SiC paper to a thickness of 0.2 to 0.3 mm, corresponding to approximately 1/μ for the glass composition (μ being the mass absorption coefficient for Cu x-rays). The polished samples were kept in a dessicator until they were used.

The thin sections which were prepared from the heat treated glasses were analyzed in a commercial Siemens Kratky camera coupled with a proportional counter and an Ortec recorder. The details of the camera described by Kratky (1954) are presented in Figures 5 and 6.

As shown in Figure 6, the beam is made very parallel in passing through the Kratky block. The size of the entrance slits used determines how near to the main beam scattering can be measured. Since the size of the scattering region is inversely related to the particle size, if the particles are large, it is necessary to use very fine slits in order to resolve them. The beam intensity is reduced considerably, however, in passing through the block. It is necessary to use an evacuated diffraction path in order to minimize air scattering.

Balanced Ni and Co filters were used to remove x-ray wavelengths other than Cu Kα. Lupolen, which is a form of paraffin, was employed in the determination of the

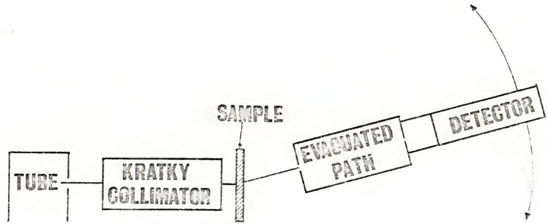

Figure 5.--Components of a Kratky small angle scattering camera.

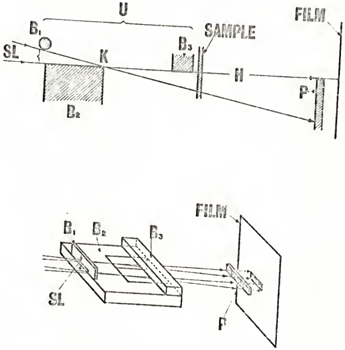

Figure 6.--Collimation system for a Kratky small angle scattering camera.

intensity of the main beam. Results were corrected for any changes in the main beam which occurred during the runs. By measuring the intensity of the beam both with and without the sample in place, the per cent transmission of each sample could be determined. Entrance slits, 150 μ in height, and exit slits, 50 μ in height, were employed for all samples. The width of the detector slit was 6 mm. The diffraction path was evacuated to 10 microns of mercury during each measurement. All of the samples were scanned from 200 μ to 700 μ above the centroid of the main beam, corresponding to 0.01° and 0.2° 2θ respectively, at a speed of 125 μ/min. The results were recorded automatically on a chart recorder at a paper speed of 2 in/min. After smoothing the curves, the intensities obtained when the Co filter was in place were subtracted from those obtained with the Ni filter. Since the samples were of various thicknesses, the data were normalized to 100% transmission of the x-ray beam in order to compare all of the curves directly.

Microscopy

Thin sections, 10-20 microns thick, were prepared from several of the partially crystalline samples by standard petrographic procedures. When these sections were viewed in transmission under polarized light, the crystals

appeared light against a dark background. Particle size determinations were made on micrographs taken of these sections by making a number of measurements of the *b* axis of the ellipsoidal crystals.

Pre-shadowed, direct carbon, replicas were made from several of the etched fracture surfaces of the glass-ceramics for use in the electron microscope. These replicas were viewed in both the Phillips EM 100 and EM 200 electron microscopes.

CHAPTER V

RESULTS AND DISCUSSION

In the first portion of this work, the kinetics of crystallization of $Li_2Si_2O_5$ from glass in the Li_2O-SiO_2 system and the mechanism of nucleation and growth were determined under various conditions. The effects of varying the nucleation treatment on the crystallization kinetics are reported. A theory relating the early stages of nucleation and growth to the bulk kinetics is also presented.

The mechanical properties of the partially crystalline glass-ceramics are then correlated with the microstructures developed by controlling the nucleation and crystallization treatments. A general theory of the strengthening effect of the crystals in the glass is presented.

Kinetics of Crystallization

In Table 3 are presented the compositions and nucleation treatments given the four series of samples investigated herein.

The results of the quantitative x-ray diffraction analyses of the kinetics of crystallization of $Li_2Si_2O_5$

TABLE 3

EXPERIMENTAL CONDITIONS AND MEASURED ACTIVATION ENERGIES

Sample Series	Composition (mole %)			Melting temp. (°C)	Nucleation treatment at 475°C (hr)	Activation energy (Kcal/mole)
	SiO_2	Li_2O	TiO_2			
A	66.7	33.3	0.0	1350	3	92
B	64.2	32.1	3.7	1350	3	77
C	66.7	33.3	0.0	1350	24	52
D	73.6	26.4	0.0	1415	3	49

are presented in Figure 7. The curves for samples B and D were normalized on a basis of the theoretical volume fraction of $Li_2Si_2O_5$ which could be crystallized from the samples. These curves are plotted on a logarithmic time scale to facilitate plotting the different temperatures together. Time was measured from the point at which the samples reached the crystal growth temperature, about 20 minutes from the time the samples were placed in the furnace. The curves are sigmoidal shaped as is normal for a nucleation and growth process. The flattening off of the curves at high percentages of crystallization probably represents the effect of impingement of the crystals in th glass, although Verduch (1958) explained the same phenomenon occurring in the formation of cristobalite from silica gel on the basis of fissures opening in the material. An incubation period, the time required to form the minimum per cent crystallinity detectable by x-ray diffraction, is present under all conditions, although this period is very short for some of the higher temperature plots. The length of the incubation period varies for the different nucleation treatments and compositions. The reason for this variation will be discussed later.

The kinetic curves show that the overall crysallization rate of $Li_2Si_2O_5$ in the temperature range of

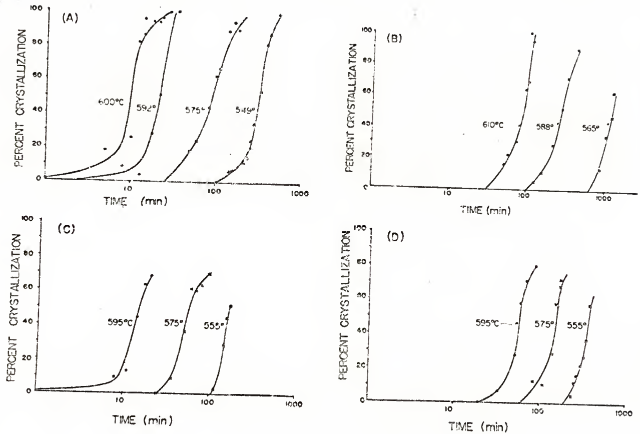

Figure 7.--Crystallization of $Li_2Si_2O_5$ from Li_2O-SiO_2 glass.

549°C-610°C is decreased by the addition of TiO_2 to the 33.3 mole % Li_2O glass (B), and the appearance of phase separation in the 26.4 mole % glass (D). However, it can be seen that the crystallization rate is increased when the nucleation time is increased (C). Much of the decrease in overall crystallization rate in the two cases cited above (B, D) can be attributed to the increase in incubation time.

It is interesting to note that most of the samples became hazy a short time before any crystallinity could be detected, suggesting that, although some crystals were present, the volume fraction was less than the limit of resolution of the diffractometer.

Another interesting feature which was noted in the x-ray diffraction patterns was the fact that samples C and D, showed a different peak orientation than did the other two sample groups. In series A and B, the most intense x-ray diffraction peak was the one corresponding to the (040) planes in the $Li_2Si_2O_5$ crystals. The peak corresponding to the (111) planes was only about one-half this height. In sample series C and D, however, it was the peak corresponding to the (111) planes which was the most intense. This result should be compared with that of Rindone (1962) in which he found that the height of the (111) peak increased with the degree of Pt nucleation in

the glass. It will be shown in a forthcoming section of this work that series C and D did undergo a greater amount of nucleation than series A and B.

The logarithm of the time to reach 50% crystallization plotted versus 1/T (°K) for the four series is shown in Figure 8. There are two obvious choices for an initial point for these plots, time = 0, or $V_v = 0$. It was decided for two resons that the latter choice, plotting from $V_v = 0$ to $V_v = 0.5$, was correct. First, a Guinier-DeWolff (1947) (1956) x-ray investigation of these glasses did not show the presence of $Li_2Si_2O_5$ until a short time before the point corresponding to $V_v = 0$. Also, as will be seen later, an analysis of the kinetics, using the Johnson-Mehl-Avrami (JMA) equation, yielded very unlikely results when the plots were made from time = 0. There is some unavoidable error present in choosing the point $V_v = 0$, however, since the diffractometer cannot accurately detect crystallinity below about $V_v = 0.05$.

By employing a typical Arhennius analysis, the slopes of the above plots yielded activation energies for the crystallization process. These activation energies are presented along with the composition and nucleation treatment given the glass in Table 3.

Essentially the same values of Q as those in Table 3 were obtained when the Arhennius type plots were made to 40 and 60% crystallization.

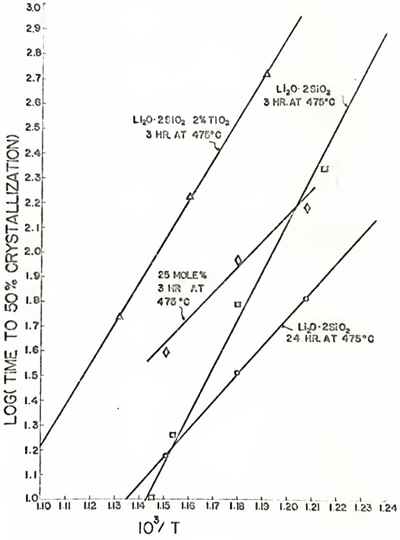

Figure 8.--Temperature dependence of the crystallization rate.

The results in Table 3 indicate that the effect of the addition of TiO_2, an increase in the nucleation time, or phase separation in the glass, is to reduce the activation energy for crystallization. As can be seen by equation (19), the measured activation energy is a complicated function of both the activation energies for nucleation and growth. It is possible to separate the activation energies of nucleation and growth, if the growth morphology (n) can be established. This can be accomplished in the following manner.

The double logarithm of V_v is plotted versus the logarithm of time during the early stages of crystallization of the four series of samples. These plots are presented in Figures 9, 10, 11, and 12. The constancy of the growth rate, necessary to obtain equation (17), which suggests this method of analysis, was substantiated by the work of Morley (1965) and Degen and Toropov (1966). These plots of the JMA equation were made from data taken from the kinetic curves given in Figure 7. The data were only plotted to $V_v = 0.5$ since above this point the effect of impingement causes the curves to change shape.

As is seen from equation (17), the slope of the curves in Figures 9, 10, 11, and 12 at low volume fractions yields a value for $(n + 1)$. The values of $(n + 1)$ along with the corresponding values of n are given in Table 4.

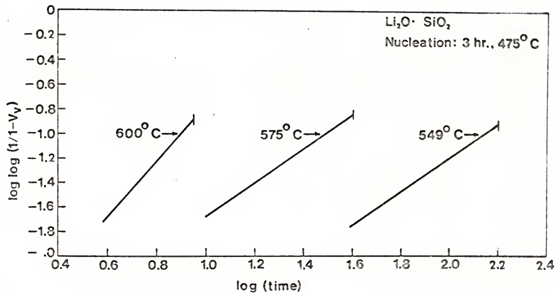

Figure 9.--Determination of the morphology of the crystallization process for series A using the JMA equation.

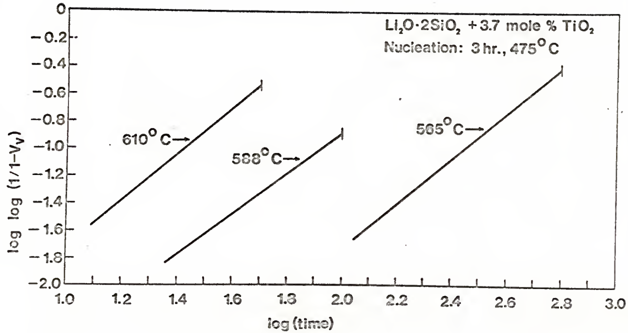

Figure 10.--Determination of the morphology of the crystallization process for series B using the JMA equation.

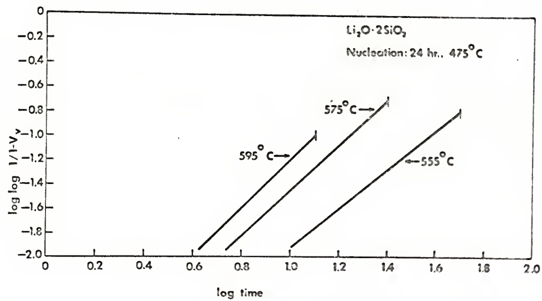

Figure 11.--Determination of the morphology of the crystallization process for series C using the JMA equation.

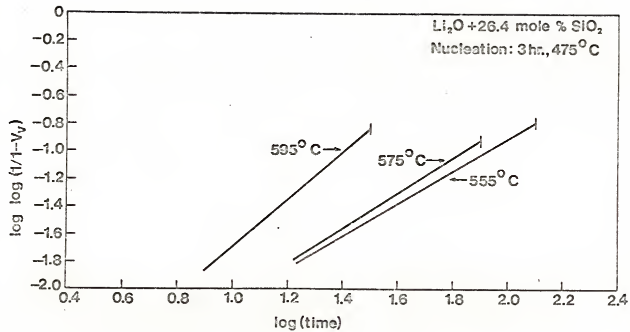

Figure 12.--Determination of the morphology of the crystallization process for series D using the JMA equation.

TABLE 4

EXPERIMENTAL SLOPES OF THE MODIFIED FORM OF THE JMA EQUATION (eq. (17))

Sample Series	Growth temp. (°C)	Slopes of eq. (17) $(n + 1)$	n
A	600	2.3	1.3
	575	1.4	0.4
	549	1.4	0.4
B	610	1.7	0.7
	588	1.5	0.5
	565	1.7	0.7
C	595	2.0	1.0
	575	1.9	0.9
	555	1.6	0.6
D	595	1.8	0.8
	575	1.3	0.3
	555	1.2	0.2

It was shown in equation (15) that the number n is determined by the morphology of crystal growth in the system. Since $n \simeq 1$ in all cases here, it can be concluded that the growth of rods is occurring.

It should be noted that most of the values of $(n + 1)$ are less than 2. The addition of the integer 1 to the value of n comes about through the integration of equation (15) where constant nucleation rate was assumed. Avrami (1941), however, showed that if the nucleation rate is not constant, but is an exponential function of time, and if nucleation occurs very quickly during the process, then the factor $(n + 1)$ reduces to n. When there is an intermediate nucleation rate, and growth is occurring in the form of rods, the slope of the JMA equation should be somewhere between 1 (very fast nucleation) and 2 (constant nucleation rate). This appears to be the case in this system.

Hillert (1958) showed that the morphology index, n, could be obtained in a different manner. He also showed that this exponent was very sensitive to the choice of the impingement factor in the rate equation. This impingement factor is of the form $(1 - V_v)^i$. Johnson and Mehl chose $i = 1$, but this value is not necessarily valid over the entire transformation range. Hillert

showed that for a generalized value of this factor, at the early stages of the transformation, that

$$\left|\frac{\partial\ \ell n\left(\partial V_v/\partial t\right)}{\partial\ \ell n\ V_v}\right|_T = 1 - \frac{1}{m} - i\ \left(\frac{V_v}{1-V_v}\right) - \frac{V_v}{RT}\ \left(\frac{dQ}{dV}\right) \tag{33}$$

At the beginning of a process, the right hand side of this expression reduces to $1 - 1/m$, and the exponent can be determined by plotting the logarithm of the slope of the transformation curve versus log V_v at these early stages, and taking the slope of this curve.

This type of analysis was applied to some of the series of samples investigated here. The plots of $\ell n\left(\frac{\partial V_v}{\partial t}\right)$ versus $\ell n\ V_v$ are presented in Figures 13 and 14. The values of m which correspond to $n + 1$ in the JMA equation, obtained from the slopes of these curves, are given in Table 5. Considering the fact that there is some difficulty in accurately measuring the slope of the transformation curve at small volume fractions, these values of m agree very well with the values of $(n + 1)$ obtained by the JMA method of analysis.

The electron micrograph of the fracture surface of the partially crystalline glass (Figure 15) and photomicrographs made from the thin sections of the glass-ceramic (Figures 16 and 17) support the analytical conclusion

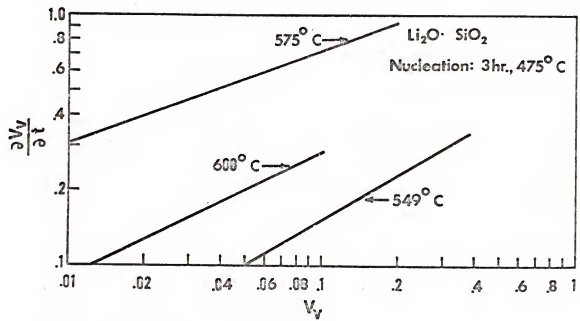

Figure 13.--Determination of the morphology of the crystallization process for series A using Hillert's method.

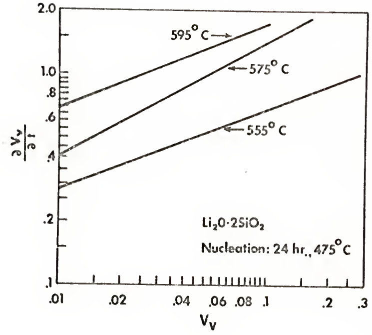

Figure 14.--Determination of the morphology of the crystallization process for series C using Hillert's method.

TABLE 5

CRYSTALLIZATION MORPHOLOGY AS DETERMINED FROM EQUATION (33) (after Hillert)

Heat Treatment				
Nucleation	Growth	Slope	m	$n + 1$ (eq. 17)
3 hr 475°C	600°C	.48	1.9	2.3
3 hr 475°C	575°C	.40	1.7	1.4
3 hr 475°C	549°C	.58	2.3	1.4
24 hr 475°C	595°C	.38	1.6	2.0
24 hr 475°C	575°C	.51	2.0	1.9
24 hr 475°C	555°C	.38	1.6	1.6

Figure 15.--Replica of a spherulite on a fracture surface of a partially crystalline sample from series A.

Figure 16.--Thin section of sample from series B, $V_v = 0.4$. (Crossed Nicols; ×350.)

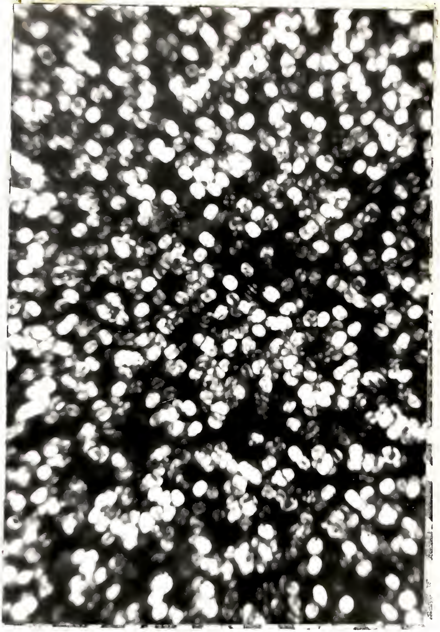

Figure 17.--Thin section of sample from series D, $V_v = 0.4$. (Crossed Nicols; ×350.)

that crystal growth occurred in the form of rods. The micrographs of the partially crystallized samples contain spherulitic crystals which are similar to those observed by Matveev and Velya (1960) and Korelova *et al.* (1964) in this system, and which are described generally by Morse and Donnay (1936). The analyses of Morse and Donnay showed that the increase in size of this form of spherulite occurs through the nucleation and growth of the individual rods that make up the crystals. They proposed that every point on the surface of a growing fibre can act as a nucleation site for a new rod. This proposition is borne out by the results of the JMA analysis and the electron micrograph in Figure 13 which more clearly illustrates the dendritic type of structure which is to be expected if new rods grow from ones already present.

Equation (19) demonstrates the fact that a rearrangement of the JMA equation can also be used to analyze the temperature dependence of both the nucleation and growth rates. If V_v in equation (19) is taken as 0.5, the plots of $\ln t_{(0.5)}$ versus 1/T are identical to the Arhennius plots shown in Figure 8. The exponential term in equation (19) suggests that what is normally measured as the temperature dependence of the glass crystallization process is actually a combination of the activation energy for nucleation and the activation energy for growth, where

the measured value depends not only on the individual activation energies, but also on the morphology of the growing phase. It should be pointed out that the growth morphology must remain constant with temperature in order for an activation energy to be measured. Since the average activation energy for the growth of $Li_2Si_2O_5$ crystals has been shown to be between 49 and 56 Kcal/mole (Morley, Degen, and Toropov, etc.), and since it was shown in this study that n at the early stages of growth does not vary appreciably, then the effect of TiO_2, phase separation or an increased nucleation time seems to be one of decreasing the activation energy for nucleation. The above factors are listed in increasing order of their effectiveness in promoting the nucleation of spherulitic rods.

Looking at the crystallization process as a whole, it is proposed that structural rearrangements tending toward the coordination of stable nuclei occur during the nucleation treatment. The type of rearrangement leading to the nucleation of the stable phase was determined by Kinser and Hench (1968) from electrical property measurements and Guinier-DeWolff x-ray diffraction studies. Their findings were substantiated by small angle x-ray scattering measurements which will be reported in the next section of

this dissertation. During the growth period, the embryos grow into stable crystals of $Li_2Si_2O_5$, but the spherulitic type nucleation and growth of rods begins only after these crystals have grown to some critical size. This fact was substantiated by the previously mentioned work of Matveev and Velya who showed that the interior of the spherulites contained a solid mass of crystals, and by the electron micrograph as shown in Figure 15, in which it is seen that the interior of the spherulites has a decidedly different structure than the exterior. Further evidence for the existence of a critical embryo size comes from the plots of the JMA equation, the sopes of which yield a physically meaningful value for the growth morphology only when the starting point is taken to be the point $V_v = 0$.

The narrow size distribution of crystals seen in the micrographs (≈ 3%) indicates that the free energy of all of the nucleation sites formed during the nucleation treatment was approximately equal and therefore all the crystal nuclei formed at nearly the same time. Increasing the nucleation time from 3 hours to 24 hours reduces the size of the crystals and increases their number per unit volume indicating that a greater degree of nucleation has occurred during the longer heat treatment.

Small Angle X-ray Scattering

X-ray diffraction is a scattering process. Most diffraction effects from a perfect crystal, sharp lines or spots, occur well separated from the direction of the main beam. It has been shown, however, that samples containing scattering heterogeneities having dimensions approximately 10 to 10,000 times that of the incident wavelength, λ, will give rise to continuous scattering in the neighborhood of the main beam.

X-ray diffraction effects are more easily explained when the reciprocal lattice concept is utilized. The reciprocal lattice of a small crystal is shown in Figure 18. Each node, h, k, l, in the reciprocal lattice corresponds to planes in the crystal having the same (h, k, l) indices. The size and shape of the node is related to the size and shape of the crystal. It is this facet of the scattering phenomenon which is of interest here. It should be noted that all nodes are identical and that there is a diffraction effect in the direction of the main beam (0, 0, 0). When the diffracting crystals are large, this peak is masked by the main beam. However, if the size of the crystal is decreased the size of the node increases proportionally, and diffraction effects extend into the region around the main beam where they may be detected.

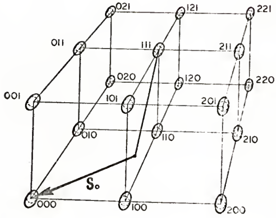

S_o = DIRECTION OF INCIDENT X-RAY BEAM. $|S_o| = \frac{1}{\lambda}$

Figure 18.--A portion of the reciprocal lattice of a small crystal.

The observation of low angle scattering is not generally possible with standard x-ray diffraction equipment since the divergence of the main beam is too great to permit low intensity observations below 3-4° 2θ. One method of limiting this divergence has been described by Kratky (1954), whose diffraction system was discussed in an earlier portion of this work.

A detailed analysis of the theory of small angle x-ray scattering has been given by Guinier (1963). Only a few of the basic relationships will be presented here.

Expressions may be developed which relate scattered intensity, I, to the scattering vector $\vec{s}$, where

$$\vec{s} = \frac{2 \sin \theta}{\lambda} = \frac{\varepsilon}{\lambda}$$

These expressions permit us to determine the various parameters which are characteristic of the scattering particles.

Near the (000) node of reciprocal space,

$$I(\vec{s}) = \frac{F^2}{VV_c} \left|\Sigma(\vec{s})\right|^2 \qquad (34)$$

where

F = structure factor; i.e. scattering power of the unit cell

V_c = volume of the unit cell

V = irradiated volume

$\Sigma(\vec{s})$ = Fourier transform of the shape function, σ, for the finite particle

It can be shown that by making the substitutions $N = V/V_c$ where N = number of unit cells, and $(F/V_c)^2 = \rho^2$ where ρ is the number of electrons/unit volume = electron density, that for a single particle containing N unit cells

$$I_N(\vec{s}) = (\rho - \rho_o)^2 |\Sigma(\vec{s})|^2 \tag{35}$$

where $(\rho - \rho_o)$ is the difference in electron density between the particle and the matrix.

From this expression, other relationships may be derived which will give information about the scattering particles.

Guinier (1963) showed that $\Sigma(\vec{s})$ at very small angles could be approximated by an exponential series. This Guinier approximation leads to equation (36) below,

$$I(s) = (\rho - \rho_o)^2 V^2 \cdot \exp \left| - \frac{4}{5}\Pi^2 r^2 s^2 \right| \tag{36}$$

Here, r is the radius of the particles which have been assumed to be spherical. The size of particles having other shapes may also be obtained. Therefore, if the logarithm of the scattered intensity is plotted as function

of the square of the scattering angle, the slope of the curve yields r^2.

Another size parameter, known as the Porod radius, can also be obtained from x-ray scattering data. Porod (1951) (1952) showed that the intensity in the tail of the scattering curve is related to the total surface area of the scattering particles, from which a particle size can be determined. Porod also demonstrated the fact that for distinct particles, the scattered intensity approached an asymptotic value at large scattering angles. This means that if log I is plotted versus log ε, the slope, in the case of a line shaped beam, should be equal to 3. This was shown to be the case for all samples measured in this study.

Gerold (1960) showed that, for spheres, the Porod radius is given by the following expression,

$$R_P = \frac{3}{8\Pi(1-V_v)} \frac{M\lambda}{\varepsilon_o^3 I(\varepsilon_o)} \tag{37}$$

where

V_v = volume fraction of scattering phase

λ = x-ray wavelength

ε_o = scattering angle

I = intensity scattered at angle ε_o

$$M = Q_o/K', \text{ where } Q_o = \text{integrated small angle and}$$
$$K' = \text{constant} = \frac{4\Pi\ell}{A\lambda^3}$$

where

$$2\ell = \text{slit length}$$
$$A = \text{distance between sample and detector}$$

The other parameter which will be considered here is Q_o, the integrated small angle intensity. Q_o has already been mentioned since it is involved in calculating the Porod radius. Guinier showed that Q_o could be described by the following relationship:

$$Q_o = 4\Pi \int_o^\infty s^2 I(s)ds = (\rho - \rho_o)^2 V_p \qquad (38)$$

where

V_p = total volume of scattering particles

One can therefore see that a change in Q_o can be caused by a change in electron concentration difference between the particles and the matrix or to a change in the volume of scattering phase.

The scattering curves obtained from the heat treated glasses plotted as log I versus ε^2 are presented in Figures 19 and 20. The presence of the humps in these curves has not been completely explained, but the major inflections which seem to occur in all of the samples are

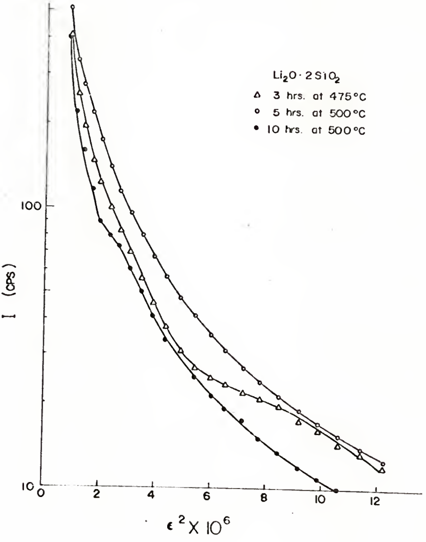

Figure 19.--X-ray small angle scattering curves from samples of 33.3 mole % Li_2O glass.

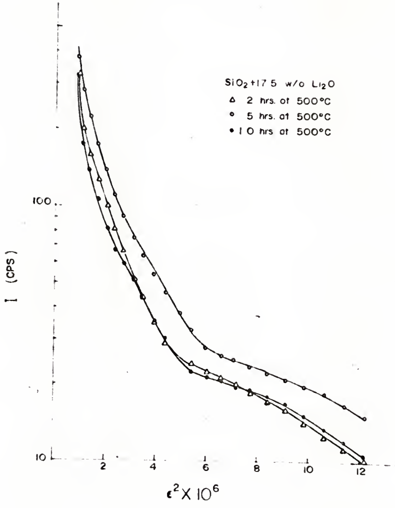

Figure 20.--X-ray small angle scattering curves from samples of 30.0 mole % Li_2O glass.

possibly due to a periodic separation between scattering centers. When a thin section rather than a bulk specimen was heat treated, the humps became more pronounced as the heat treatment progressed. Actual peaks developed at certain angles as the stable crystalline phase began to appear.

The slope of the curves in the small angle region where the function is nearly a straight line gives a measurement of the Guinier radius (R_G) of the particles. The scattering particles were assumed to be spherical, and the radii were determined using equation (36). In cases, where more than one straight line portion of the curve occurred a range of radii were calculated. This phenomenon is common in cases where a particle size distribution is present. The values of the Guinier radius are listed in Table 6 along with the values for the Porod radius which were calculated using equation (37). Because the intensity approached an assymptotic value at large angles, the value of M in equation (37), a measure of the total integrated intensity could be calculated using a computer program designed by Gould (1968). It was necessary to assume a value for V_v, the volume fraction of scattering phase. From Guinier-DeWolff x-ray diffraction data, Kinser and Hench (1968) determined the scattering phase to be lithium metasilicate (Li_2SiO_3). The volume fraction

TABLE 6

PARTICLE SIZES OBTAINED FROM X-RAY SMALL ANGLE SCATTERING

Guinier Radius R_G (Å)			Porod Radius R_p (Å)		
Heat Treatment Time-Hours	30 Mole % Li_2O	33.3 Mole % Li_2O	Heat Treatment Time-Hours	30 Mole % Li_2O	33.3 Mole % Li_2O
2	265-302		2	159	
3		256	3		162
5	228-272	233	5	149	196
10	237-310	242	10	143	194

was approximately 0.001. Variations in volume fraction in this range are not critical to the accurate determination of R_p.

It should be noted from Table 6 that R_p is always smaller than R_G. This is to be expected because R_p is based on the total surface area of the particles, and is therefore weighted toward the smaller particle sizes. It is this fact which normally allows one to determine the particle size distribution from this method. However, in this case, R_p and R_G are so nearly alike that a distribution would have little meaning.

The most important feature to notice in these results, however, is that neither the Guinier radius nor the Porod radius changes significantly with heat treatment time. This is consistent with the work of Goganov and Porai-Koshits (1965) who also found R_G to be essentially constant with heat treatment. The meaning of these results in terms of a structural model will be discussed later.

The other measured parameter which provides information regarding the early stages of the crystallization process was the total integrated intensity, Q_o. The values of M which are related to Q_o through the relation $Q_o = M/K'$ is plotted versus the time at 500°C in Figure 21. The two curves, representing the two compositions investigated,

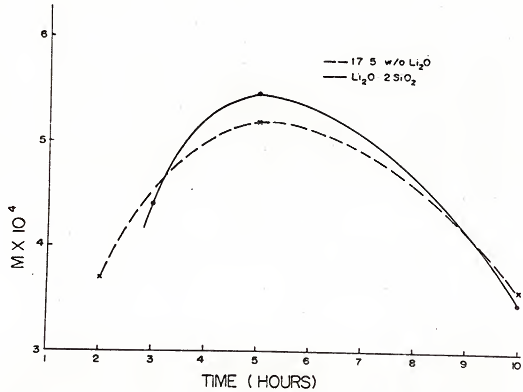

Figure 21.--Variation in integrated scattered intensity with heat treatment time at 500°C.

30.0 and 33.3 mole % Li_2O, both contain a maximum in scattered intensity at a time of 5 hours.

From equation (38) it can be seen that this scattering maximum can be due to two things, an increase in the total volume of scattering phase, or an increase in the electron density difference between the scattering phase and the matrix. Since neither the particle size, not the size distribution changes with time, as evidenced by the constancy of both the Guinier and Porod radii, a change in $\Delta\rho$ must be occurring.

The maximum in scattering corresponds to the same time at which Kinser and Hench found maxima in the dielectric loss angle (tan δ), while measuring the electrical properties of these glasses. The tan δ maxima were determined to be present in the samples which were used for the small angle scattering measurements. Kinser and Hench explained the maxima in loss angle in terms of the growth and dissolution of a metastable lithium metasilicate phase. This conclusion is supported by the findings obtained by small angle x-ray scattering. The difference in electron density between the Li_2SiO_3 phase and the $Li_2Si_2O_5$ matrix produces the maxima in scattered intensity. As the Li_2SiO_2 disappears, so does the amount of scattering. Since, only a compositional change and not a geometrical change is going on within the glass, the unchanged size of the

cellular glassy structure is not surprising. The electron micrographs of an as cast and a heat treated glass contained in Figures 22 and 23 support the SAS results in regard to the size of the scattering regions.

Relation of Nucleation to Bulk Crystallization

The next question to be answered is how the appearance of metastable Li_2SiO_3 influences the kinetics of crystallization of the stable $Li_2Si_2O_5$ phase. As was seen previously, changing the nucleation time from 3 to 24 hours both increased the crystallization rate and decreased the activation energy for nucleation. Electrical measurements made on the glass nucleated for 24 hours indicated the presence of lithium metasilicate, while a 3 hour treatment did not produce Li_2SiO_3. This fact combined with the effect of the heat treatment on the nucleation rate and activation energy led to the conclusion that the lithium metasilicate which forms during this period acts as the nucleating agent for the stable lithium disilicate. It is not so strange that Li_2SiO_3 should crystallize before the expected $Li_2Si_2O_5$. Kalinina and Filipovich (1964) came to the conclusion that lithium metasilicate rich regions were present in glass of essentially the same composition as that studied here. Vogel (1960) has established the presence of secondary

Figure 22.--Fracture surface of as cast 30.0 mole % Li_2O glass.

Figure 23.--Fracture surface of 30.0 mole % Li_2O glass heat treated 10 hours at 500°C.

phase separation in other glasses. The simplicity of the metasilicate structure compared to the disilicate structure is apparently the basis for the preferential nucleation of Li_2SiO_3. Once the metasilicate is present, it is easy to see from the schematic of the two structures in Figure 24 how the disilicate can be formed from metasilicate by diffusion of alternate Li_2O groups out of the structure.

It is this diffusional step which is responsible for the incubation period. When a critical disilicate crystal size is reached, spherulitic growth begins, and crystallization occurs rapidly. Spherulitic growth is probably preferred because of the ease of diffusion of Li_2O from the ends of the dendrite arms.

When the nucleation heat treatment is sufficient to produce the ordered metasilicate, the spherulite size is smaller and the number of crystals per unit volume is larger than when the metasilicate is absent. Besides producing the metasilicate crystals, the longer nucleation period also results in regions around the crystals which are more ordered than the glass. The nucleation of spherulitic rods is more favorable in these ordered regions than in the nonordered glass, and the nucleation activation energy is lowered.

It was noted that the incubation time for the 3.7 mole % TiO_2 samples was especially long. It is theorized

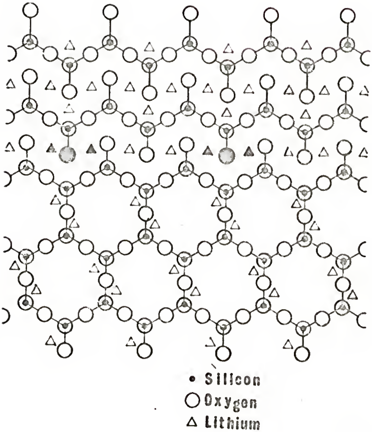

Figure 24.--Schematic diagram of $Li_2Si_2O_5$ and Li_2SiO_3 structures.

that this increase in the incubation period is due to a change in the nucleation mechanism from internal activation by metastable Li_2SiO_3 to nucleation by Ti^{+4} ions. Since it was shown by Nakagawa and Izumitani (1968), that at large concentrations of TiO_2 (22 w/o), that Li_2O-TiO_2 crystals are the nucleating agents in the glass, it appears likely that at low concentrations of TiO_2 a transition in nucleation mechanism occurs, so that neither method is particularly effective.

The basis for internally activated nucleation may be seen thermodynamically if one looks at equation (6) which gives the hetergeneous nucleation rate as a function of temperature. As mentioned previously, at large degrees of supercooling such as occurs in the crystallization of glass, ΔF_a governs the rate of crystallization. It is easy to see that ordering around the metasilicate regions should reduce the energy barrier to transfer a molecule from the glassy to the crystalline state, thereby reducing the activation energy for nucleation.

Even when no metasilicate has been formed during the nucleation treatment, the activation energy of the incubation time for crystal growth remains the same because the diffusional step to form the nuclei of the equilibrium phase must still occur. An "activation energy

for incubation" was determined from the Arhennius plots in Figure 25 to be 100 Kcal/mole in both cases. The spherulites, once formed, however, do not envelop ordered regions, and the nucleation activation energy is high.

Mechanical Properties

In this section of the dissertation, the effect of crystallization on the elastic modulus, coefficient of thermal expansion, and the fracture strength of partially crystalline lithia-silica glass-ceramic specimens will be reported. The fracture strength measurements will be discussed with respect to their dependence on particle size and volume fraction of crystals and the nucleation heat treatment given the glass. The results will be analyzed quantitatively in terms of the various theories of strengthening which were discussed in the introductory portion of this work.

Elastic Modulus

The results of the measurements of the modulus of elasticity versus per cent crystallization are presented in Figure 26. As expected, the modulus of the glass having the higher per cent SiO_2 has a larger elastic modulus. Also as expected, the values of the modulus for

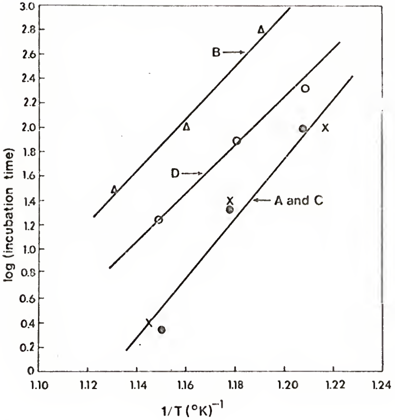

Figure 25.--Temperature dependence of the incubation time.

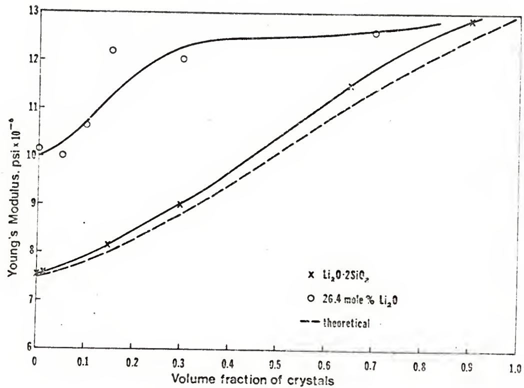

Figure 26.--Variation of Young's modulus with crystallization.

the two compositions approach each other at large percentages of crystallization. The measured values of the modulus of the partially crystalline Li_2O-SiO_2 composition were compared with those predicted by expressions proposed by Hashin and Shtrikman (1962). The measured values of E and the values of ν_{glass} and $\nu_{crystal}$ determined by Bokin *et al.* (1965) were used in Hashin's equations to obtain the theoretical variation of modulus with crystallinity. This theoretical curve is shown as the dashed line in Figure 26. Due to the large scatter in measured values of the modulus of the 26.4 mole % glass, no attempt was made to correlate these values with the theory. The values of the modulus for the glass and the crystals do agree fairly well, however, with moduli determined by Bokin *et al.* for samples of nearly the same composition.

Coefficient of Thermal Expansion

The coefficient of thermal expansion determined at several percentages of crystallization is plotted versus the volume fraction of crystals in Figure 27. The experimental curve is compared with that theoretically predicted by Kingery (1960) for the coefficient of thermal

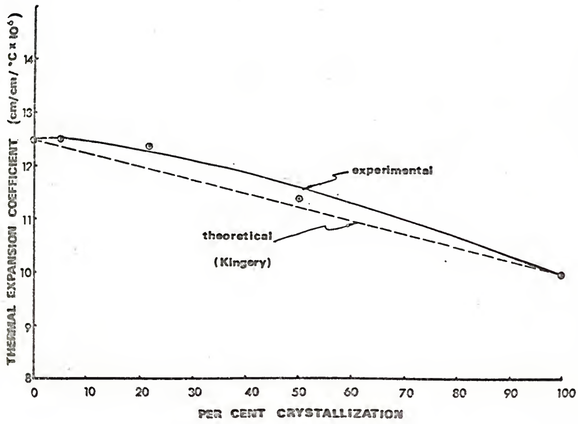

Figure 27.--Variation of thermal expansion coefficient with crystallization.

expansion in multiphase bodies. The expression relating thermal expansion coefficient to the relative amount of the two phases is presented below.

$$\alpha = \frac{\alpha_1 w_1 K_1/\rho_1 + \alpha_2 w_2 K_2/\rho_2}{K_1 w_1/\rho_1 + K_2 w_2/\rho_2} \qquad (39)$$

where

α = thermal expansion coefficient

K = bulk modulus of the given phase

w = weight fraction of the given phase

ρ = density

If the Poisson's ratio of the two phases is nearly the same, which was true in this study, the Young's modulus can be used in place of bulk modulus. It can be seen that agreement between the theoretically predicted and the experimental values are fairly good.

Fracture Strength

Of principal interest in this investigation was the influence of crystallization and especially nucleation treatment on the fracture strength of the partially crystallized glass-ceramics. It will be shown that the

information gained from the studies of the model glass-particle systems can be applied toward understanding the more complicated glass-ceramics.

The diametral compression test was used to measure the fracture strength. This test provides a means of measuring the relative strengths of the various samples. The fairly low strengths which were obtained imply that fracture was initiated at the end surfaces of the specimens. If microcracks in the interior of the samples were controlling the fracture process, strengths over an order of magnitude greater should have been obtained.

Three types of fracture were observed. At low volume fractions of crystals, the samples exploded into many pieces at fracture. This phenomenon was explained by Kenny (1957) as due to the reflection of the elastic waves which propagate as fracture occurs. The more highly crystalline samples either fractured along the diameter of the samples, or broke in the triple cleft pattern described by Rudnick, Hunter and Holden (1963). No evidence of shear or compressive failure at the sample surfaces was ever observed. Even though some unevenness of the cylindrical surfaces of the samples was present, observations of the loading pads after fracture had occurred showed that pressure had been applied uniformly over the length of the samples.

The fracture strengths of the glass-ceramics are plotted versus the volume fraction of $Li_2Si_2O_5$ crystals in Figure 28. Each point represents the arithmetic average of about twelve specimens. The error in the determination of the average strength was approximately ± 10% within 95% confidence limits. Most of the interest was centered on the understanding of the effect of nucleation treatment on the strength of the type of glass-ceramic produced from glass of the Li_2O-$2SiO_2$ composition. The strength of the 26.4 mole % Li_2O glass was also measured for various volume fractions of crystals. The strength of the Li_2O-$2SiO_2$ composition to which approximately 0.2% Pt had been added was also investigated. The glass itself was grayish due to the presence of the large amount of colloidal Pt. An electron micrograph taken from a fracture specimen of this glass is shown in Figure 29. It was found that in opposition to the results reported by Rindone (1962), who claimed that the addition of large amounts of Pt prevented crystallization, the glass of this composition crystallized to a volume fraction of 0.75 in approximately 30 minutes at 575°C without the benefit of any nucleation heat treatment. Crystallization was very homogeneous.

Two interesting features can be noted in Figure 28. The first is the increase in the degree of strengthening

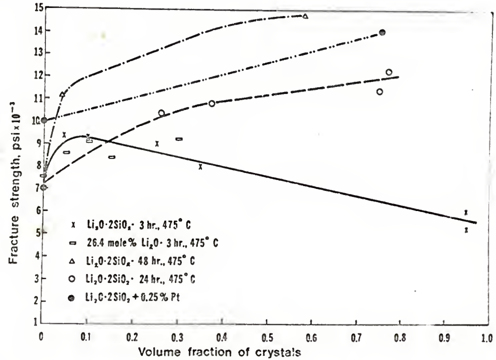

Figure 28.--Dependence of fracture strength on volume fraction of crystals for several nucleation treatments.

Figure 29.--Fracture surface of an as cast Li_2O-$2SiO_2$ glass to which 0.25 % Pt has been added.

by the second phase crystals as the nucleation time is increased. The second is the fact that for the 3 hour treatment, the strength actually decreased at volume fractions greater than 0.1. These observations will be explained a little later.

It is difficult to compare these results of Figure 28 with those obtained by other investigations since few studies have been carried out in which strength was measured as a function of volume fraction of crystals, or even as a function of time at a given temperature. As mentioned before, Davis (1966) attributed the strength decrease in a multicomponent glass-ceramic to flaws opened in the glass-ceramic due to the anisotropic thermal expansion of the crystalline phase. Ownby (1962) and Watanabe *et al.* (1962) showed that the strength of a glass-ceramic was highly dependent on the heat treatment schedule employed during the crystallization process.

Results obtained from a number of model glass-particle systems are similar in appearance to these data. Studt and Fulrath (1962), Binns (1962), and Nason (1963) demonstrated that an initial increase in strength accompanying the addition of crystals to a glass was followed by a decrease in strength at large volume fractions. This decrease was proposed to be due to

cracks opening in the composite because of stresses on the particles, or because of lack of bonding of the particles to the glass.

Both the strength increase and the decrease at high volume fractions for the short nucleation treatment must be explained. These explanations will be given separately.

There are a number of ways in which the presence of second phase crystals can increase the strength of a composite. These are listed below.

1. Increase in Young's modulus with per cent crystallinity; strength increases in proportion to $\sqrt{E}$.

2. Random reduction of flaw length; $\sigma = \sigma_o(1-V_v)^{-1/2}$

3. Decrease in particle size; $\sigma \approx (p)^{-1/2}$

4. Reduction in flaw length due to reduction in mean free path between particles; $\sigma \approx (\lambda)^{-1/2}$

It is possible to eliminate the first three of these factors because they will not account for the degree of strengthening which occurs. For instance, at the point at which a strength of 11,300 psi at 10% crystallinity is measured, a combination of factors (1) and (2) will predict a strength of only 8000 psi. At any given volume fraction of crystals, the change in particle size from a

3 to a 48 hour nucleation treatment is insufficient to account for the degree of strengthening. There is approximately a 60% decrease in particle size between the 3 hour and 48 hour nucleation treatments. There is no evidence that at the volume fractions at which the largest strengthening occurs that fracture is initiated within the crystals.

Hasselman and Fulrath (1966) suggested a strengthening mechanism which can account for the strengths which were measured herein. As shown previously, they demonstrated that the strength of a brittle composite varied as $\lambda^{-1/2}$, where λ is the mean free path between particles. In this study, since the particles were elliptical in shape, λ is given by

$$\lambda = \frac{4(k_1 b)(1 - V_v)}{3V_v} \tag{40}$$

where

b = one-half the minor axis of the ellipse

k_1 = constant determined by the ratio of the major to the minor axis of the ellipse, DeHoff (1964); a/b remained constant at 1.6 through all treatments

The strength should vary as $\lambda^{-1/2}$ only in the region in which, $\lambda < c$, where c is the flaw size in the glass. One can calculate c from the Griffith relation

given in equation (21). Here γ is assumed to be 3000 ergs/cm^2 (Wiederhorn, 1968), E was measured to be 7.5×10^6 psi, and the strength of the glass was determined to be 7×10^3 psi. A value of c of 85 microns was calculated.

A plot of measured fracture strength versus $\lambda^{-1/2}$ is presented in Figure 30. The region in which σ is proportional to $\lambda^{-1/2}$ is represented by the heavy line. This region occurs above a flaw size of 75 microns, which is in good agreement with the calculated value of 85 microns. Considering the ± 10% error in strength and the error in measuring both volume fraction and particle size, the fit is very good. Below a mean free path of 75 microns, the increase in strength of the glass-ceramic over the uncrystallized glass can be accounted for by factors (1) and (2). The deviations from the theory at large λ's will be explained in the next section.

As in the case of strengthening mechanisms, there are a number of factors which can contribute to the reduction in strength of the glass-ceramics at high volume fractions. These factors are listed below.

1. Stresses around particles due to thermal expansion coefficient differences between crystals and glass.

2. Stress concentrations around crystals due to a difference in elastic moduli between phases.

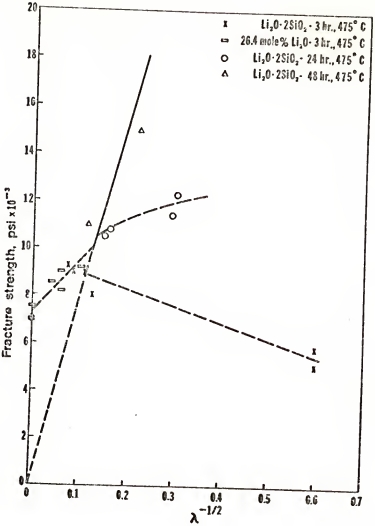

Figure 30.--Variation of the fracture strength of the glass-ceramics with mean free path between crystals.

3. Stresses due to a difference in volume between crystals and glass.

The stresses due to thermal expansion coefficient differences were calculated from Selsing's expression (equation (24)). The measured value for E and α were employed along with values of ν_g and ν_p obtained by Bokin *et al.* (1965). A maximum radial compressive stress of 8000 psi and a tensile tangential stress of 4000 psi was calculated. These stresses, however, are independent of particle size, and should also be independent of nucleation treatment, so that they cannot explain the differences in strengths.

The stress concentrations due to differences in elastic moduli were calculated from the expressions given by Goodier (1933). Because the elastic modulus changed only by a factor of 2 during crystallization, the stress concentration was only 1.2. This stress is also independent of particle size.

It was determined that the only stresses which could produce effects which would be dependent on nucleation treatment were those stresses arising from the density difference between glass and crystals. Since a maximum density change of from 2.30 (3 hour nucleated glass) to 2.45 (crystals) can occur, a large amount of

strain can be produced during crystallization. Theoretically, of course, crystallization takes place at temperatures above the softening point of the glass. It was seen, however, that at crystal volume fractions as low as 0.3 the softening point of the specimen increased to 600°C as shown in Figure 31. This means that the amount of stress which can be relieved is reduced as the mean free path between crystals is lowered. It is expected that as the nucleation time is increased, the degree of mismatch between crystals and glass, and therefore the magnitude of the stress produced during the crystallization process is reduced. Bonding between the crystals and the glass should also be improved as the nucleation period is lengthened. These volume differences, unlike the thermal expansion coefficient differences, should produce very large radial tensile stresses. The type of fracture which occurs and which is shown in the electron micrographs of Figures 32 and 33 provides further evidence of these radial tensile stresses. It is seen that fracture proceeded through the spherulitic crystals, rather than around them as would be expected if the tangential stresses were controlling fracture. This type of fracture was noted exclusively on all fracture specimens investigated.

Density studies were conducted in order to determine the effect of the stresses arising from

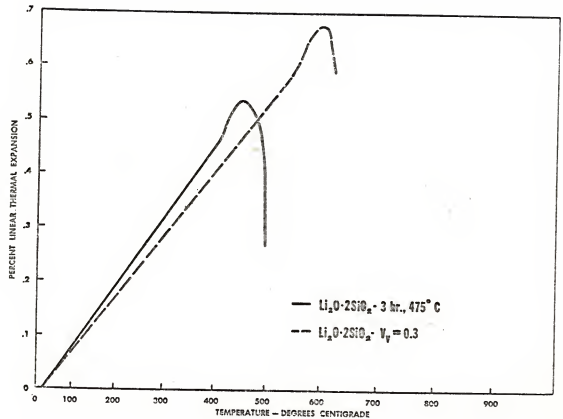

Figure 31.--Softening points of nucleated and partially crystalline Li_2O-SiO_2 glass.

Figure 32.--Fracture surface of partially crystalline sample from series A.

Figure 33.--Fracture surface of partially crystalline sample from series C.

volumetric changes accompanying crystallization. These studies consisted of weighing a sample in both air and water, and employing Archimedes' principle to determine the density.

The studies provided a number of interesting results. It was first discovered that increasing the nucleation time increased the density of the glass from 2.30 gm/cc (3 hour) to 2.33 gm/cc (24 hour), to 2.34 gm/cc (48 hour), indicating that rearrangement processes are going on during this treatment. The density of a number of partially crystalline samples was also measured. It was found that the measured densities did not correspond to those which should have been found had the samples been 100% dense. The theoretical densities were determined on the basis of a glass density of 2.35 gm/cc, a crystal density of 2.45 gm/cc, and the assumption that density should vary directly as the volume fraction of crystals. The value of 2.35 gm/cc was measured in a glass that had been heat treated at 575°C for a time just before any crystallization would occur. The discrepancies in density measurements provide the clue by which the fracture strength differences can be understood.

Studt and Fulrath (1962) showed that the strength of mullite-glass compacts could be described by two functions, one dependent on particle size, the other

dependent on the amount of porosity in the system. It was discovered that the same sort of analysis could be applied to the results determined herein.

The expression relating fracture strength to mean free path between crystals and the volume fraction of porosity in the sample is given in equation (41) below.

$$\sigma = K\lambda^{-1/2}e^{-bP} \tag{41}$$

where

$K = \sqrt{4E\gamma/\Pi}$

b = empirical constant

P = volume fraction of porosity = 1 - measured density/theoretical density

It was shown that the porosity varied as $\lambda^{-1/2}$ in Figure 34. The fact that porosity varies with λ is expected since the smaller the mean free path between crystals, the less stress relaxation should occur in the glass. There is no explanation at present for the particular variation of porosity with λ. A calculated value of b of 50 was shown to hold over the entire range of strengths and nucleation treatments. That is, by multiplying the function containing the amount of porosity times the strength predicted by the $\lambda^{-1/2}$ relation all of the experimental strength curves will be reproduced. The value of b obtained in this study is large compared to

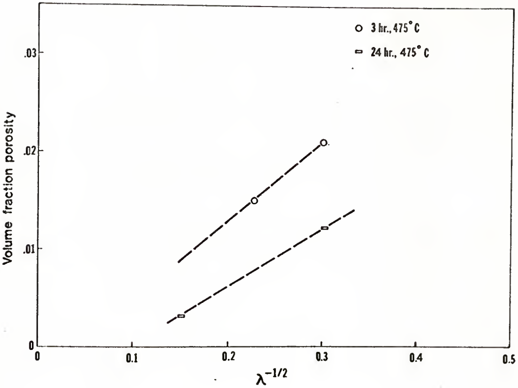

Figure 34.--Dependence of the porosity in the partially crystalline samples with mean free path between crystals.

that determined by Studt and Fulrath, probably because the porosity is present in the glass-ceramics as cracks rather than holes so that its effect on the strength is more pronounced. The decrease in porosity with an increase in nucleation time is shown very clearly in Figures 35 and 36. It is seen that the 3 hour nucleated specimen is much more cracked than the 48 hour sample, where both have been crystallized to obtain the same mean free path between particles.

In summary then, it has been shown that the elastic modulus increased with crystallization while the thermal expansion coefficient decreased. It was demonstrated that the crystals in the glass strengthened the composite by reducing the average flaw size. It was shown that the maximum degree of strengthening by the crystals is attained only in a 100% dense body, and that the lack of strengthening in the less nucleated samples can be attributed to porosity, where the porosity occurs because of stresses produced between the more dense crystals and the glass during crystallization.

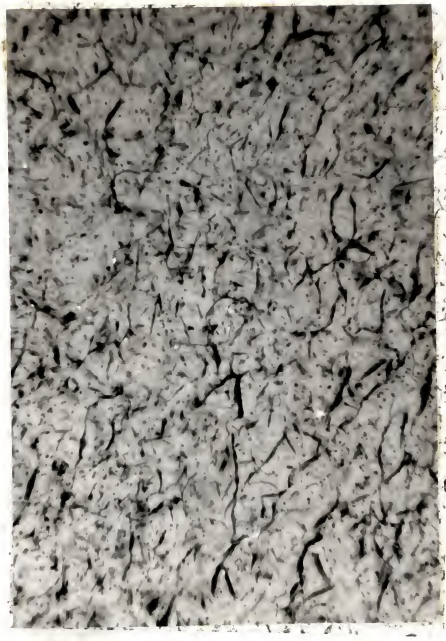

Figure 35.--Thin section of partially crystalline glass which had been nucleated 3 hours at 475°C. (Uncrossed Nicols; ×350.)

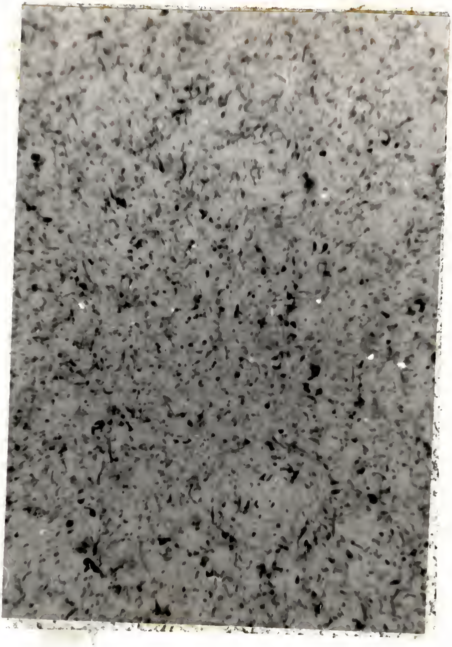

Figure 36.--Thin section of partially crystalline glass which had been nucleated 48 hours at 475°C. (Uncrossed Nicols; ×350.)

CHAPTER VI

SUMMARY AND CONCLUSIONS

A number of conclusions can be drawn from the results of this investigation. These are given below.

1. It was shown that an increase in nucleation time from 3 to 24 hours, the addition of TiO_2, or phase separation results in a decrease in the activation energy for crystallization.

2. It was also shown that of the above factors, the increase in nucleation time increased the crystallization rate, but the other factors decreased this rate.

3. It was effectively demonstrated that both the Johnson-Mehl-Avrami equation and an equation given by Hillert could be used to predict that crystal growth in this system occurred in the form of rods.

4. By employing a modified form of the JMA equation it could be concluded that the reduction in measured activation energy mentioned in point (1), was due to a reduction in the activation energy for nucleation.

5. Micrographs of the partially crystalline samples showed that crystal growth was spherulitic in nature.

6. Small angle x-ray scattering studies confirmed the conclusions of other investigators that enhanced nucleation after larger heat treatment times at 475°C was due to the presence of a metastable phase.

7. It was concluded that the strengthening effect of the second phase crystals was due to the reduction in flaw size in the glass.

8. It was also concluded that the deviation of the strength below that predicted by the strengthening theory was due to cracking in the composite, where this cracking occurred because of stresses set up between the crystals and the glass during crystallization.

9. It was concluded that increased nucleation in the glass reduced the cracking by providing better bonding between the glassy and crystalline phases.

It would be of interest at this point to consider the results of this study in more general terms.

The results of the investigation into the kinetics of crystallization have emphasized a number of important

points. The first of these points is the fact that the addition of a "so called" nucleating agent is not always necessary in order to promote homogeneous crystallization. In fact, as was seen in the case of the addition of TiO_2 to the Li_2O-SiO_2 glass, nucleation can actually be retarded by addition of these nucleating agents. There is also evidence which supports the contention that many different types of nucleation, some more favorable than others, can exist in the same glass composition. It was apparent in this investigation, for instance, that the addition of Pt enhanced crystallization much more than the internal activation mechanism, which in turn was more favorable than the addition of TiO_2. It was also shown in this study that it is the nucleation step which controls the microstructure of the ensuing glass-ceramic. It is through this bridge of microstructure that we can begin to understand the effect of nucleation and crystallization on the properties of the glass-ceramic.

Enhanced nucleation in the glass can affect the microstructure of the glass-ceramic in a number of ways. More effective nucleation produces a larger number of sites from which crystal growth is energetically more feasible, resulting in a smaller final particle size in the material. A quantitative comparison of the microstructures developed in samples nucleated for 3 hours

or 24 hours showed that the longer nucleation increases the relative number and decreases the size of the crystals in the Li_2O-SiO_2 samples. It was also shown that another effect of nucleation was to promote the formation of a more dense, less cracked, glass-ceramic. It is theorized that the improved structure is due to the more coherent bonding between the crystals and the glass, and to the reduction in stress between the phases.

It should be emphasized that it is the final microstructure that is important in determining the properties of the material, and not the method of obtaining this microstructure. Different nucelation treatments which will produce the same microstructure will have the same effect on the properties. It was shown in this study that equivalent microstructures could be obtained from either internally activated nucleation or Pt nucleation in the Li_2O-SiO_2 glasses.

The microstructural effects discussed in the previous paragraphs play a primary role in determining the mechanical properties of the composite. It was shown, for instance, that cracking in the samples due to less effective nucleation of the crystals almost completely destroyed the strengthening effect of the second phase particles. One can also see that if the strengthening mechanism is the limiting of flaw size by the crystals,

that at any volume fraction of particles, a reduction in crystal size produces a similar reduction in mean free path, and therefore an increase in strength. Similarly, an increase in the volume fraction of crystals of any size produces an increase in strength, provided no other mechanisms are acting. More effective nucleation of the crystals can produce the smaller particle sizes, and can ensure that little reduction in strength will occur due to cracking of the composite.

The microstructure itself may be complicated by a number of factors which were not considered in this study. For instance, more than one crystalline phase can appear during heat treatment (Davis, 1966); large compositional differences may exist between the glassy and crystalline phases; crystal size distributions can occur; crystal shapes may be very complicated; and the crystals themselves may be very anisotropic.

All of these factors may be taken into account, however, through the interaction of the stress fields with the microstructural features in the sample. The same list of factors which were discussed with respect to the results obtained in this program can be employed to determine the most effective strengthening and weakening mechanisms in other glass-ceramics. Whether the same

choice of controlling mechanisms will be made depends on the particular system chosen.

Using the information gained during this study, and the results of other investigators, it is theoretically possible then to optimize both nucleating and crystallization conditions in a particular glass system in order to produce a glass-ceramic having the most desirable properties.

CHAPTER VII

SUGGESTIONS TO FUTURE INVESTIGATORS

1. A study should be made into the possibilities of developing a test for the strength of bulk glass which would be independent of surface condition. One suggestion toward this end would be to modify the diametral compression test so that the stresses at the ends of the cylinder are eliminated. This could possibly be accomplished by either producing a cylinder having hemispherical ends, or by loading the cylinders over only a portion of their length. Another suggestion is the use of the thermal quench test on glass spheres in which the surface of the spheres are in hydrostatic compression and the interior in tension.

2. The bonding between the crystals and the glass in glass-ceramic materials should be investigated since it is the bonding which plays a major part in determining the final properties of the samples.

3. X-ray diffraction should be employed to measure both the microstresses and the macrostresses produced during crystallization. Both of these stresses can be obtained from a line profile analysis of the diffraction peaks of the crystalline phase.

4. The role of nucleating agents such as Pt, TiO_2, ZrO_2, and others in the production of the glass-ceramic microstructures should be studied more thoroughly.

5. X-ray radial analysis should be carried out during the crystallization process. This analysis could provide the answer as to the nature of the transformations which are occurring during crystallization.

6. Transmission electron microscopy should be performed in order to provide more information regarding the structure of the partially crystallized glasses. The most effective means of preparing thin sections for transmission seems to be by ion bombardment of the material.

APPENDIX

APPENDIX I

RESULTS OF TEST CONDITION VARIATION ON STRENGTHS MEASURED USING THE DIAMETRAL COMPRESSION TEST

A short study was conducted to determine the effect of changes in the test atmosphere, loading speed, and variation in annealing treatment on the measured fracture strength of glassy and partially crystalline samples using the diametral compression test.

The diametral compression test was conducted in air at loading speeds of 0.2 and 0.02 inches/min, corresponding to times to failure of approximately 10 and 100 sec respectively. The samples employed were 33.3 mole % Li_2O glass which had been nucleated for three hours at 475°C, but not annealed. It was found that within 95% confidence limits of ± 10%, there was no difference in strength measured at the two speeds. This result indicates that static fatigue may not be a major factor in this type of test, since normally a modulus rupture reduction of up to 25% has been reported (Shand, 1954) accompanying this same increase in loading time.

Tests were also conducted under H_2O rather than in air. A 10% reduction in strength was noted in this case. This decrease, nevertheless, is also less than normally reported from results of modulus of rupture tests.

It was also noted that the effect of annealing the glassy and partially crystalline samples at 440°C followed by a furnace cool was to decrease the strength of all of those specimens by approximately 15%. This decrease can be explained on the basis of the presence of a residual stress distribution in the glass samples before annealing. Kingery (1960) has shown that a fast quench from temperatures above the glass transformation point can produce a tensile stress in the center and a compressive stress in the surface of a piece. Since fracture is most likely initiated at the sample ends, a compressive stress in this region should tend to increase the applied stress necessary to propagate a flaw.

BIBLIOGRAPHY

Avrami, M., 1939, *J. Chem. Phys.*, 7, 1103.

Avrami, M., 1941, *J. Chem. Phys.*, 9, 177.

Berenbaum, R. and Brodie, I., 1959, *Brit. J. Appl. Phys.*, 10, 281.

Binns, D. B., 1962, *Science of Ceramics*, 1, 315 (Academic Press).

Bokin, P. Ya. *et al.*, 1965, *The Structure of Glass*, 5, 126 (Consultants Bureau).

Brown, S. D. and Ginell, R., 1962, *Symposium on Nucleation and Crystallization in Glasses and Melts*, 109 (American Ceramic Society).

Burke, J. E. and Turnbull, D., 1952, *Prog. Met. Phys.*, 3, 220.

Caniero, F., 1947, *Reunion des Laboratoires d'Essai des Materiaux*, Paris.

Charles, R. J., 1958, *J. Appl. Phys.*, 29, 1657.

Davis, R. F., 1966, *Govt. Report AD 638 336*.

Degen, M. G. and Toropov, N. A., 1966, Translated from *Izvestiya Akademii Nauk. SSR, Neorganicheskie Materialy*, 2, 1617.

DeHoff, R. T., 1964, *Trans. AIME*, 230, 764.

DeHoff, R. T., 1968, private communication.

DeWolff, P. M., 1947, *Appl. Sci. Res.*, B1, 119.

Douglas, R. W. and Mohyuddin, J., 1960, *Phys. Chem. Glasses*, 1, 71.

Fine, M. E., 1952, *ASTM, STP No. 129*.

Fine, M. E., 1964, *Introduction to Phase Transformations in Condensed Systems*, 13 (Macmillan).

Fletcher, N. H., 1958, *J. Chem. Phys.*, 29, 572.

Frenkel, J., 1946, *Kinetic Theory of Liquids*, 415 (Claredon Press).

Frey, W. J. and Mackenzie, J. D., 1967, *J. Materials Science*, 2, 124.

Fullman, R. L., 1953, *Trans. AIME*, 197, 447.

Fulrath, R. M., 1959, *J. Am. Ceram. Soc.*, 42, 423.

Gerold, V. K., 1961, *Physica Status Solidi*, 1, 37.

Goganov, D. A. and Porai-Koshits, E. A., 1965, *The Structure of Glass*, 5, 82 (Consultants Bureau).

Goodier, J. N., 1933, *J. Appl. Mech.*, 1, 39.

Gould, R. W., 1968, private communication.

Griffith, A. A., 1921, *Phil. Trans.*, A221, 163.

Grossman, L. N., 1961, M. S. Thesis, University of California, Berkeley.

Guinier, A., 1956, *Theory et Technique de la Radiocrystollographie* (Dunod).

Guinier, A., 1963, *X-ray Diffraction* (Freeman).

Gurney, C. and Pearson, S., 1952, *Ceramics and Glass*, 10, Govt. Reports, Ministry of Supply, London.

Hashin, Z. and Shtrikman, S., 1962, *J. Mech. Phys. Solids*, 10, 335.

Hasselman, D. P. H. and Fulrath, R. M., 1966, *J. Am. Ceram Soc.*, 49, 68.

Hasselman, D. P. H. and Fulrath, R. M., 1967, *J. Am. Ceram. Soc.*, 50, 399.

Hench, L. L., 1967, *Proceedings of the Fourth Space Congress*, Cocoa Beach, Florida.

Hillert, M., 1958, *Acta Met.*, 7, 653.

Hillig, W. B. and Turnbull, D., 1956, *J. Chem. Phys.*, 24, 914.

Inglis, C. E., 1913, *Trans. Inst. Naval Arch.*, 55, 219.

Jaccodine, R. J., 1961, *J. Am. Ceram. Soc.*, 44, 472.

Jacobson, L. A., 1962, M. S. Thesis, University of California, Berkeley.

Johnson, W. A. and Mehl, R. F., 1939, *Trans. AIME*, 135, 416.

Kalinina, A. M. and Filipovich, V. N., 1964, *The Structure of Glass*, 3, 53 (Consultants Bureau).

Kenny, W. J., 1957, M. S. Thesis, University of Minnesota, Minneapolis.

Kingery, W. D., 1960, *Introduction to Ceramics* (Wiley).

Kinser, D. L. and Hench, L. L., 1968, *J. Am. Ceram. Soc.*, 51, 445.

Korelova, A. I., Degen, M. G., and Alekseeva, O. S., 1964, *Structure of Glass*, 3, 65 (Consultants Bureau).

Kratky, O., 1954, *Zeitschrift fur Electrochemie*, 58, 49.

Kuznetsov, A. V., 1959, *Zh. fiz Khimii*, 33, 1492.

Matsuda, J. and Suito, E., 1964, *Kogyo Kagaku Zasshi*, 67, 884.

Matveev, M. A. and Velya, V. V., 1960, *Glass Ceram.*, 16, 543 (Eng. Transl.).

McMillan, P. W., 1964, *Glass-Ceramics* (Academic Press).

McMillan, P. W., Phillips, S. V., and Partridge, G., 1966, *J. of Materials Science*, 1, 269.

Moore, R. E., 1962, Ph.D. Thesis, University of Missouri, Rolla.

Morley, J. G., 1965, *Glass Technol.*, 6, 77.

Morse, H. W. and Donnay, J. D. H., 1936, *Am. Mineralogist*, 21, 391.

Mould, R. E. and Southwick, R. D., 1959, Presented at the Annual Meeting—Am. Ceram. Soc., Chicago.

Munch, R. H. and Pierron, E. D., 1963, *Norelco Reptr.*, 10, 75.

Nakagawa, K. and Izumitani, T., 1968, *Vi Symposium on Basic Ceramics in Japan*, Osaka.

Nason, D. O., 1963, M. S. Thesis, University of California, Berkeley.

Ohlberg, S. M., Golob, H. R., and Strickler, D. W., 1962, *Symposium on Nucleation and Crystallization in Glasses and Melts*, 55 (American Ceramic Society).

Ownby, P. D., 1962, M. S. Thesis, University of Missouri, Rolla.

Phillips, S. V. and McMillan, P. W., 1965, *Glass Technol.*, **6**, 46.

Porod, G., 1951, 1952, *Kolloid Z.*, **124**, 83; **125**, 51 and 109.

Preston, F. W., Baker, T. C., and Glathart, J. L., 1946, *J. Appl. Phys.*, **17**, 162.

Reaumur, M., 1739, *Memoires de L'Academie des Sciences*, 370.

Rindone, G. E., 1962, *J. Am. Ceram. Soc.*, **45**, 7.

Rindone, G. E., 1962, *Symposium on Nucleation and Crystallization in Glasses and Melts*, 63 (American Ceramic Society).

Roy, R., 1962, *Symposium on Nucleation and Crystallization in Glasses and Melts*, 39 (American Ceramic Society).

Rudnick, A., Hunter, A. R., and Holden, F. C., 1963, *Materials Research and Standards*, **3**, 283.

Ruiz-Menacho, C. and Roy, R., 1959, *Bull. Am. Ceram. Soc.*, **38**, 229.

Selsing, J., 1961, *J. Am. Ceram. Soc.*, **44**, 419.

Shand, E. B., 1954, *J. Am. Ceram. Soc.*, **42**, 276.

Stookey, S. D., 1956, Brit. Patent No. 752,243.

Stookey, S. D., 1959, *Glastech. Ber.*, V International Glass Congress, 32K, Heft V.

Stookey, S. D. and Meaurer, R. D., 1962, *Progress in Ceramic Science*, **3**, 77 (Pergamon Press).

Studt, P. and Fulrath, R. M., 1962, *J. Am. Ceram. Soc.*, 45, 182.

Tammann, G., 1925, *The States of Aggregation* (Van Nostrand).

Tashiro, M., Sakka, S., and Wada, M., 1960, *J. Ceram. Assoc. Japan*, 68, 65.

Tashiro, M., 1966, *Glass Industry*, 428.

Turnbull, D., 1956, *Solid State Physics*, 3, 252 (Academic Press).

Turnbull, D. and Cohen, M. H., 1960, *Modern Aspects of the Vitreous State*, 45 (Butterworth).

Verduch, A. G., 1958, *J. Am. Ceram. Soc.*, 41, 427.

Vogel, W., 1960, *The Structure of Glass*, 2, 24 (Consultants Bureau).

Vogel, W. and Gerth, K., 1962, *Symposium on Nucleation and Crystallization in Glasses and Melts*, 11 (American Ceramic Society).

Watanabe, M., Caporali, R. V., and Mould, R. E., 1962, *Symposium on Nucleation and Crystallization in Glasses and Melts*, 23 (American Ceramic Society).

Welch, J. H., 1956, *Proc. Third International Conference on the Reactivity of Solids*, 677, Madrid.

Wiederhorn, S. M., 1968 (to be published), *Proc. of the Symposium on Mechanical and Thermal Properties of Ceramics* (Gaithersburg, Maryland).

Wright, P. J. F., 1955, *Mag. Concrete Res.*, 7, 87.

BIOGRAPHICAL SKETCH

Stephen W. Freiman was born January 21, 1942, in Alexandria, Louisiana. His early education was obtained in Pineville, Louisiana. In 1959, he was graduated from Menard Memorial High School, Alexandria, Louisiana. The author entered the Georgia Institute of Technology in September, 1959, receiving a Bachelor of Chemical Engineering in June, 1963, and Master of Science in Metallurgy in June, 1965. He entered the University of Florida in September, 1965, and received a Doctor of Philosophy in 1968. Upon receiving his degree, Mr. Freiman will be employed by the Illinois Institute of Technology Research Institute.

The author is a member of the American Institute of Mining, Metallurgical, and Petroleum Engineers, American Society for Metals, American Ceramic Society, Society of Glass Technology, and ΑΣΜ.

This dissertation was prepared under the direction of the chairman of the candidate's supervisory committee and has been approved by all members of that committee. It was submitted to the Dean of the College of Engineering and to the Graduate Council, and was approved as partial fulfillment of the requirements for the degree of Doctor of Philosophy.

December, 1968

Robert E. Uhrig
____
Dean, College of Engineering

____
Dean, Graduate School

Supervisory Committee:

____
Chairman

F. N. Rhines
____

____

____

J. B. Conklin Jr.
____